Studies on a robust method for estimating rice canopy transpiration based on the heat balance model and its application

2021

Rintaro Kondo

Contents

Abbreviations

Symbol	Description	Unit
C_p	Heat capacity of air	J g^{-1} °C^{-1}
d	Zero-plane displacement	m
E	Canopy transpiration rate	g m^{-2} s^{-1}
E_{NN}	Canopy transpiration rate predicted by the model based on neural network	g m^{-2} s^{-1}
e_a	Vapor pressure of air	hPa
$e^*(T_c)$	Saturated vapor pressure at temperature T_c	hPa
G	Soil heat flux density	W m^{-2}
g_c	Canopy diffusive conductance	m s^{-1}
H	Sensible heat flux density	W m^{-2}
r_a	Aerodynamic resistance	s m^{-1}
r_a'	Aerodynamic resistance by the original heat balance model	s m^{-1}
r_a*	Aerodynamic resistance under windless conditions	s m^{-1}
R_h	Radiation from heater	W m^{-2}
R_n	Net radiation	W m^{-2}
RH	Relative humidity of air	%
T_a	Air temperature	°C
T_c	Canopy surface temperature	°C
U	Wind velocity	m s^{-1}
z	Altitude	m
z_0	Ground roughness length	m

γ	psychrometric constant	hPa $°C^{-1}$
κ	von Karman's constant	(no unit)
λ	Latent heat of vaporization	J g^{-1}
ρ	Air density	kg m^{-3}

Chapter 1

Introduction

1.1 Demand and challenges for rice yield improvement

The world population has reached approximately 7.7 billion in 2019 and is estimated to be grown up to 10.6 billion in 2050. The global calorie supply should be approximately doubled by 2050 from 2010 level (Keating et al., 2014). Rice (*Oryza Sativa* (L.)) has been used as a primary food in the most part of Asia and Africa. These two regions account for a 76.8 % of global populations in 2019, and their population growth rate from 2020 to 2050 is estimated to be 1.58 % per year (United Nations, 2019). However, the rice yield in 2019 is 2.2 t ha^{-1} in Africa and 4.5 t ha^{-1} in Asia except East Asia, while is 7.0 t ha^{-1} in East Asia (FAO, 2019). Additionally, future expansion of cultivated acreage will be limited because of ongoing urbanization and desertification. Therefore, an increase of total production and yield per unit area of rice is a prime task for us.

In 1960s, appearance of high-yielding cultivars such as IR8, released by International Rice Research Institute (IRRI), and spread of cultivation techniques occurred, known as Green Revolution. The key point of this innovation is an introduction of a semi-dwarf characteristic, which prevented lodging and enabled high input of nitrogen fertilizers and improve harvest index (Yoshida, 1972; Evans, 1993; Peng and Khush, 2003). This innovation much contributed to an increase of rice yield more than double from 1960 to 2000 (Khush, 2001). Green Revolution was followed by a breeding of hybrid rice and new plant type (NPT) rice. The characteristics of first-generation NPT

rice is represented by large panicles, low-tillering capacity, and dark green leaves (Peng et al., 1994). Although yield of first-generation NPT rice was disappointing because of its poor grain filling, second-generation NPT rice achieved higher yield than conventional *indica*-inbred varieties. In second-generation NPT rice, greater grain filling and disease and insect resistance was derived from *indica* germplasm. Hybrid rice has been grown since 1973 in China and since 1978 at IRRI. The yield advantage of hybrid rice was approximately 15 % in China (Yuan, 1994) and 9 % at IRRI (Peng et al., 1999). Hybrid rice has a great biomass productivity, leaf area expansion, and efficient sink formation (Yamauchi, 1994; Laza et al., 2001; Kabaki, 1993). It is reported that hybrid rice showed higher yield than NPT rice because of its higher biomass production, larger size of panicles, and greater grain filling (Yang et al., 2007).

The yield of field crops is determined by the product of harvest index and total biomass production, and harvest index almost reached its upper limit (Evans, 1993; Mann, 1999; Horton, 2000). Future improvement of rice yield potential may be realized mainly by an increase of biomass production (Peng et al., 2000). The dry matter production can be determined by the product of solar radiation, light interception efficiency, and radiation use efficiency (Monteith, 1977; Long et al., 2006). Among these factors, light interception efficiency is thought to have very limited capacity for further improvement (Beadle & Long, 1985). Hence, further studies are needed especially on radiation use efficiency for improving yield in rice.

1.2 Photosynthesis under changing environmental conditions

Photosynthesis is the basic process for biomass production in plants. Many studies on the mechanisms, activity, and relationship of photosynthesis with biomass and yield

have been conducted, with both positive (Long et al., 2006; Zhu et al., 2010; Wu et al., 2019; Yoon et al., 2020) and negative (Takai et al., 2013) conclusions about this relationship being reached. Photosynthetic activities are much affected by meteorological conditions. For instance, strong radiation accelerate photosynthesis under favorable temperature conditions (Choudhury, 1987; Yamori & Hikosaka, 2014), while net photosynthetic rate decreases under high-temperature conditions (Yin et al., 2010; Khan et al., 2013; Crafts-Brandner and Salvucci, 2002; Salvucci and Crafts-Brandner, 2004). The humidity of air affects the stomatal aperture and transpiration rate (Morison & Gifford, 1983; Monteith, 1995) and drought stress also suppresses photosynthetic activities (Chen et al., 2011; Carmo-Silva et al., 2012; Mutava et al., 2015). Recently, response of photosynthesis to fluctuating light has being intensively studied (Qu et al., 2016; Taylor & Long, 2017; Vialet-Chabrand & Lawson, 2019; Shimadzu et al., 2019; Kimura et al., 2019). For example, the natural variations of photosynthetic induction responses have been reported in rice (Yamori et al., 2016; Adachi, Tanaka et al., 2019), soybean (Tanaka et al., 2019; Soleh et al. 2016), wheat (Salter et al., 2019), and cassava (De Souza et al., 2019). A majority of these studies are focused on photosynthetic activities in a single leaf under steady or simply fluctuating environmental conditions. However, field crops are grown as canopies under continuously and randomly changing meteorological conditions, and there have been less information about canopy photosynthetic capacities under field conditions. Under such situations, gas exchange is affected by various factors which is not considered in a majority of previous studies (e.g., mutual shading of leaves, aerodynamic resistance of canopies, wind velocity, plant types). Therefore, continuous measurement of canopy gas exchange with short intervals and evaluation of canopy gas exchange under various meteorological conditions is needed to

improve our understandings of biomass production process in field-grown rice.

1.3 Evaluating canopy gas exchange

Some methods to evaluate canopy photosynthesis have been developed. Models to estimate canopy photosynthetic rate based on single leaf photosynthetic rate and light irradiance have been established (Monsi & Saeki, 2005; Johnson & Thornley, 1984; Anten, 1999). The eddy covariance (Ohtaki, 1984; Alberto et al., 2014), assimilation chambers (Drake & Leadley, 1991; Katsura et al., 2006; Burkart et al., 2007; Song et al., 2016), and satellite imagery (Sebrin et al., 2015) have been also utilized to evaluate the canopy photosynthetic activity.

The thermal imaging technique is a powerful tool for evaluating canopy photosynthesis, because leaf transpiration is remarkably well correlated to its surface temperature (Gates, 1968; Jones, 2014). Additionally, recent devices of thermal imaging are compact enough to be handheld, so are very suitable for taking measurements in field conditions. Monteith & Unsworth (2013) established a model to evaluate heat balance of the canopy based on its surface temperature. Based on Monteith's theory, many studies on canopy heat transfer have been conducted. Horie et al. (2006) estimated canopy diffusive conductance (g_c) under field conditions and revealed that g_c is correlated with leaf stomatal conductance, crop growth rate during the 2-week period before full heading, and final grain yield in rice. Recently, methods of continuous estimation of canopy transpiration rate using thermal imaging in soybean (Hou et al., 2019) and cotton (Jones et al., 2018) have been developed. However, the majority of these measurements have dealt with values at an instantaneous moment or with long time intervals between measurements. The temporal resolution of these existing techniques is not sufficient to

evaluate the non-steady state of photosynthesis. In the field, meteorological conditions including solar radiation, air temperature, and relative humidity are randomly changing. Consequently, canopy photosynthesis and transpiration are dramatically changing and in non-steady state in many cases. Therefore, for comprehensive understandings of canopy gas exchange under field conditions, continuous estimations of canopy gas exchange with short intervals are needed. To achieve this objective, we need to develop a method with high stability and time-resolution.

1.4 The objective of the present study

The objective of the present study was to evaluate the canopy gas exchange under fluctuating meteorological conditions for gaining better understanding of the process of biomass production in rice under field conditions.

In Chapter 2, a stability of the heat balance model was improved by a modification based on an analysis of aerodynamic characteristics in rice canopies. The stability of the modified heat balance model was evaluated through the sensitivity analyses to the meteorological conditions. In Chapter 3, the diurnal and daily changes of canopy transpiration of field-grown rice varieties was monitored. Genotypic differences of cumulative canopy transpiration and a relationship between yield were also discussed. In Chapter 4, the required variables for estimating rice canopy transpiration were decreased to save labor costs for necessary measurements. A model to predict rice canopy transpiration rate only from meteorological data was established using the neural networks. For training and evaluation of this model, cumulated data throughout the 3-years recordings of canopy transpiration rate by the modified heat balance model was used. Based on the developed model based on neural networks, the response of rice

canopy transpiration to combinations of various meteorological factors and its genotypic difference were evaluated.

Chapter 2

Development of a method of stable estimation of rice canopy transpiration

2.1 Introduction

The stability of Monteith's original heat balance model is an issue of concern when canopy transpiration rate (E) is estimated in short time intervals. The model estimation of E results in very high or even negative values when wind velocity is very low, while it is stable under breezy conditions. This is due to the assumption in Monteith's model that the aerodynamic resistance strongly depends on the wind velocity. Because the wind velocity is quite unstable in field conditions, it is very difficult to apply Monteith's original heat balance model to continuous measurements in short time intervals in the field.

The aim of this study was to develop a method sufficient enough for estimation of rice canopy transpiration under field conditions. The heat balance model was modified based on the aerodynamic characteristics in rice canopies. After the modification, the stability of the original and modified heat balance model was compared.

2.2 Theory

The E can be calculated based on the energy balance model. In Monteith's model, the energy balance of a crop canopy can be given as:

$$R_n = H + \lambda E + G \quad \dots (1)$$

where R_n is the net radiation flux density (W m^{-2}), H is the sensible heat flux density (W m^{-2}), λ is the latent heat of vaporization (2442 J g^{-1}), E is the evapotranspiration rate (g m^{-2} s^{-1}), and G is the soil heat flux density (W m^{-2}). When the rice canopy fully covers the

land surface, it can be assumed that $G \approx 0$ and E nearly equals the canopy transpiration rate (Sakuratani & Horie, 1985). Then H can be shown as:

$$H = \frac{C_p \rho (T_c - T_a)}{r_a} \quad \ldots (2)$$

where C_p is the heat capacity of air (1.006 J g^{-1} °C^{-1}), ρ is the air density (1.204 kg m^{-3}), T_c is the canopy surface temperature (°C), T_a is the air temperature (°C), and r_a is the aerodynamic resistance (s m^{-1}). The r_a is shown as:

$$r_a = \frac{ln\{(z-d)/z_0\}^2}{\kappa^2 U} \quad \ldots (3)$$

where z is the altitude (m), d is the zero-plane displacement (0.7*canopy height, m), z_0 is the ground roughness length (0.13*plant height, m), κ is the von Karman's constant (0.4), and U is the wind velocity at altitude z (m s^{-1}). In Eq. 2 and 3, all the terms can be measured or are already known. Therefore, E can be calculated by:

$$E = \frac{(R_n - H)}{\lambda} \quad \ldots (4)$$

For calculating canopy diffusive resistance (s m^{-1}), the following equation was used:

$$\lambda E = \frac{C_p \rho \{e^*(T_c) - e_a\}}{\gamma (r_a + r_c)} \quad \ldots (5)$$

where $e^*(T_c)$ is the saturated vapor pressure at temperature T_c (hPa), e_a is the vapor pressure of air (hPa), γ is the psychrometric constant (0.662 hPa °C^{-1}), and r_c is the canopy diffusive resistance. In Eq. 5, all the terms except for r_c can be calculated or are already known. Therefore, from Eq. 5, r_c can be determined by:

$$r_c = \frac{C_p \rho \{e^*(T_c) - e_a\}}{\gamma \lambda E} - r_a \quad \ldots (6)$$

A reciprocal of r_c is the canopy diffusive conductance (g_c, m s^{-1}):

$$g_c = \frac{1}{r_c} \quad \ldots (7)$$

However, in Eq. 3, when $U = 0$, r_a diverges, then $H \approx 0$ and $R_n \approx \lambda E$. This means that

there is no heat exchange between the canopies and the atmosphere and is a major cause of errors in g_c and E estimation. Hence, to apply Monteith's model to g_c and E estimation under field conditions, a modification is needed.

To enable the continuous estimation of g_c and E under field conditions, we assumed the existence of aerodynamic resistance under windless conditions (r_a*). After the evening, the $\lambda E \approx 0$ because stomata are almost closed. In well-developed rice canopies, it can be assumed that $G \approx 0$. Therefore, Eq. 1 in the evening can be written as follows:

$$R_n = H \quad \ldots (8)$$

A part of the canopy was surrounded by silver sheet having approximately 1 m height to block the wind and heat transfer from the side of the canopy (Fig. 2.1a). The surrounded plants were heated with an infrared heater for a few minutes until the canopy reached thermal equilibrium (Fig. 2.1b). In equilibrium state, the sum of radiation from the heater (R_h) and R_n equaled to H. Averaged R_n during the heater experiment is used for the following calculation. The radiation by the heater is separately measured as a function of the distance (Fig. 2.1c). Based on this relationship, R_h is calculated from the distance of heater and rice canopy. Therefore, the heat balance of the rice canopy can be shown by:

$$R_h + R_n = H = \frac{C_p \rho (T_c - T_a)}{r_a^*} \quad \ldots (9)$$

Consequently, the r_a* can be given by:

$$r_a^* = \frac{C_p \rho (T_c - T_a)}{R_h + R_n} \quad \ldots (10)$$

When the net radiation is negligible, T_a can be assumed to be equal to T_c before being heated (T_{c0}). Therefore, the Eq. 10 can be converted to Eq. 11.

$$r_a^* = \frac{C_p \rho (T_c - T_{c0})}{R_h + R_n} \quad \ldots (11)$$

The modified r_a was then defined as the combined resistance of r_a calculated by the

original heat balance model (r_a') and r_a*.

$$r_a = \frac{1}{\frac{1}{r_a'}+\frac{1}{r_a^*}} \quad \ldots (12)$$

With this modification, the divergence of r_a under windless conditions can be avoided because of the existence of r_a* regardless of the wind velocity.

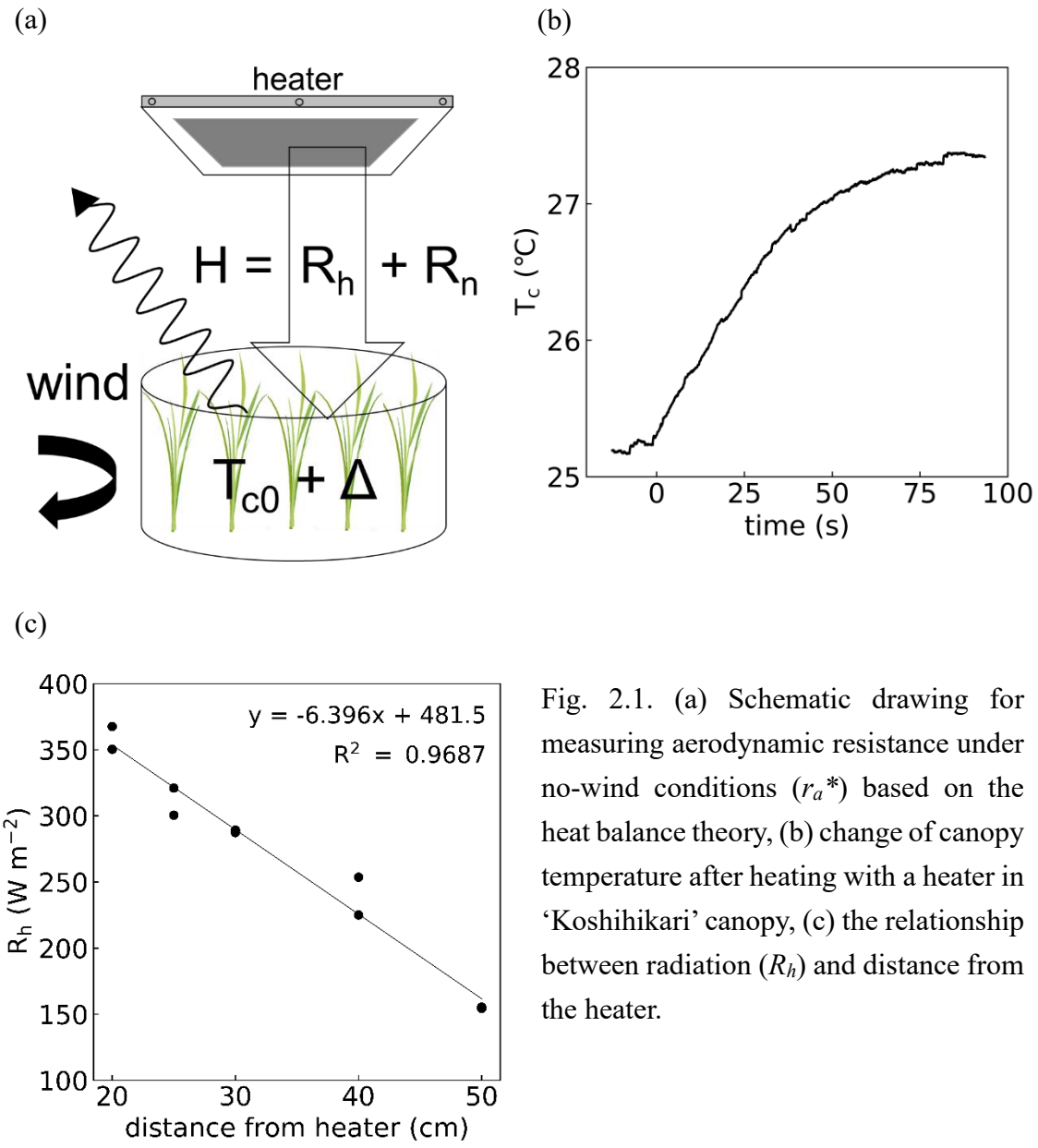

Fig. 2.1. (a) Schematic drawing for measuring aerodynamic resistance under no-wind conditions (r_a*) based on the heat balance theory, (b) change of canopy temperature after heating with a heater in 'Koshihikari' canopy, (c) the relationship between radiation (R_h) and distance from the heater.

2.3 Materials and Methods

2.3.1. Plant materials

The field experiments were conducted in the paddy field at the Graduate School of Agriculture, Kyoto University, Kyoto, Japan (35° 2′ N, 135° 47′ E, 65 m altitude). Seven rice genotypes were cultivated; 'Koshihikari', 'Nipponbare' (typical *japonica* cultivars having moderate photosynthetic activities), 'Takanari', 'Habataki' (high yielding *indica* cultivars having high photosynthetic activities), 'Wanlun 422' (a typical *indica* cultivar, WL), 'Liaojing 5' (an erect panicle type cultivar, LG) and 'IL23' (one of the recombinant inbred lines derived from a cross between 'Wanlun 422' and 'Liaojing 5', having low stomatal conductance; Tang et al., 2017; Oishi et al., 2015). The seeds were sown on April 20, 2017, and the seedlings were transplanted on May 16, 2017. Planting density was 22.2 plants m^{-2}. For aerodynamic resistance under windless condition (r_a*) measurement, 8 by 6 plants were used. The amounts of fertilizer applied as basal-dressing were 60 kg N ha^{-1}, 47 kg P ha^{-1} and 56 kg K ha^{-1}. Weeds, diseases, and insects were strictly controlled, and the field was fully irrigated throughout the entire growing season. Canopy height and leaf area were measured on July 15, 2017, with 3 replications.

2.3.2 The r_a measurement*

The measurement of r_a* of each rice genotype was conducted during the evening of July 19 with three replications at the paddy field. 3 × 3 plants were surrounded by a silver sheet and the surrounded plants were heated by infrared heater "Dantotsu" (Midori Shokai, Japan). The R_h was estimated based on the distance between the heater and the canopy, and the relationship shown in Fig. 1c. The canopy surface temperature was recorded by thermal imaging camera CPA-T620 (FLIR systems Inc., US) set approximately 1m away

from the canopy. The resolution of thermal image was 640 × 480 pixels, the spectral range was 7.5 ~ 14 μm and thermal sensitivity was 0.04 ˚C at 30 ˚C. The change of the canopy surface temperature during the heating was extracted using thermal imaging software FLIR tools + (FLIR systems Inc.). The emissivity of canopy was set as 1.0. During the measurement of r_a*, upward and downward radiation were recorded by an albedo meter (PCR-3, Kipp & Zonen, Netherlands) and infrared radiometer (PRI-01, PREDE CO., Ltd., Japan). The R_n was calculated as the sum of subtraction of upward and downward radiation of long- and short-wave radiation. These instruments were set approximately 2 m above the ground (1 m above the canopy), connected to a data logger (CR-1000, Campbell Scientific, Inc.), and the values were logged in 1 second intervals. From R_h, R_n, and canopy surface temperature, the r_a* was calculated based on the theory above.

2.3.3. Sensitivity analysis of the modified model

To test the stability of the modified model to the wind velocity and other meteorological conditions, a sensitivity analysis was conducted. Parameters in the model were fixed as T_a = 30 °C, RH = 65 %, R_n = 700 W m^{-2}, canopy height = 0.7 m and r_a* = 20 s m^{-1}, respectively. Wind velocity and canopy temperature depression (T_c-T_a) varied from 0 to 5 m s^{-1} and -2 to 0 °C, respectively, and g_c was calculated based on both Monteith's original model and the modified model for all the combinations of wind velocity and T_c-T_a.

2.3.4. Statistical analysis

The r_a* was represented by the mean value of 3 replications. An analysis of variance (ANOVA) and Tukey HSD test was used to compare variance in r_a*. The statistical

analyses were conducted using R (R Core Team, 2018). The sensitivity analysis was conducted using Python language (Van Rossum & Drake, 2009).

2.4 Results

Significant varietal differences of r_a* were observed (Fig. 2.2a), with r_a* ranging from 9.50 to 35.40 s m^{-1} among the genotypes. The relationship between r_a and wind velocity on July 20 for both the original and the modified model is shown in Fig. 2.2b. In the original model, r_a ranged up to 154.15 s m^{-1} when wind was very weak (0.36 m s^{-1}). On the other hand, r_a modified by r_a* ranged up to 8.95 s m^{-1} under weak-wind conditions. The values of leaf area index (LAI) and canopy height (CH) in each cultivar is shown in Table 2.1. The value of r_a* was significantly correlated to leaf area density, which is represented by the ratio of leaf area index to canopy height (Fig. 2.3).

With this modification, our model was applicable to a wider set of weather conditions than the original model (Fig. 2.4). In the original model, g_c estimation when wind velocity is under 3.0 m s^{-1} was unstable. This resulted in values of g_c being extremely high or even negative in some cases (Fig. 2.4a). In contrast, our modified model was capable of stable g_c estimation even when wind velocity is remarkably low (Fig. 2.4b). It should be noted that we recorded no negative values (black area) in our revised model. On the other hand, g_c estimation when wind velocity is over 3.0 m s^{-1} did not differ significantly between the two models.

2.5 Discussion

Significant varietal differences of r_a* among the seven genotypes were detected (Fig. 2.2a). This difference can be attributed to canopy structure differences of each genotype.

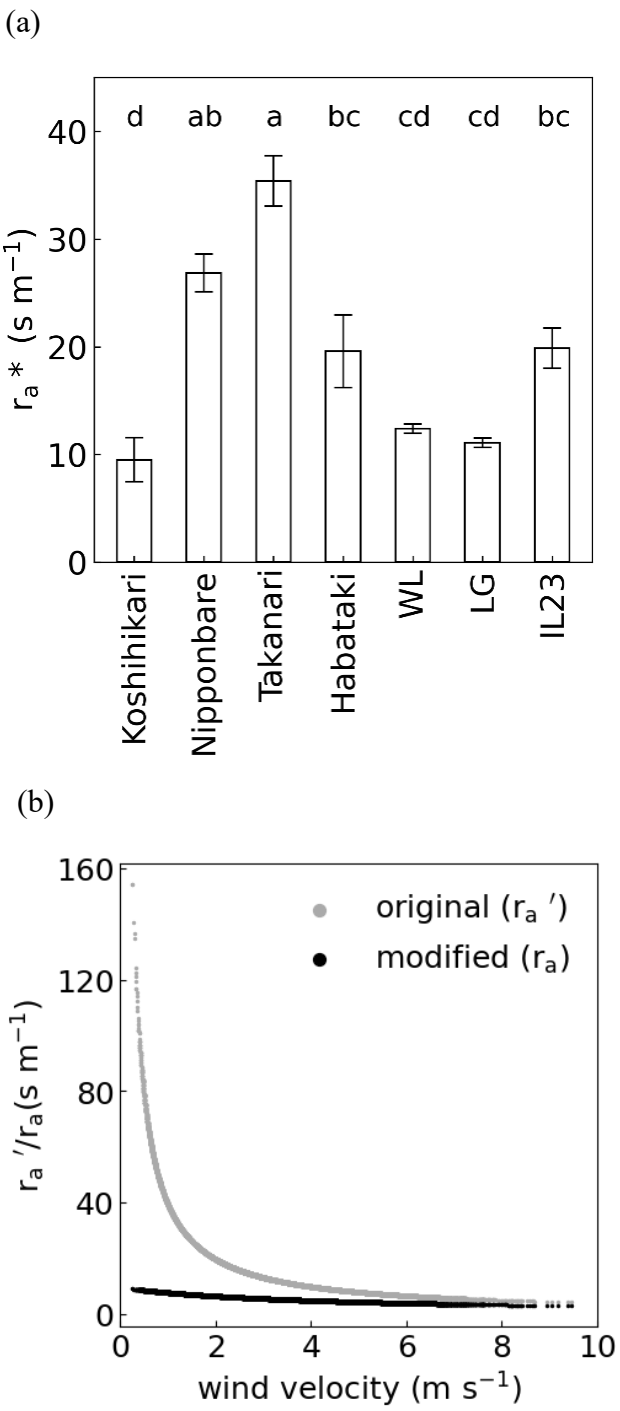

Fig 2.2. (a) Varietal differences in aerodynamic resistance under windless conditions (r_a*) measured by the method shown in Fig. 2.1. Error bars represent standard error and lowercases represent significant differences with p = 0.05 probability level by Tukey HSD test in 3 replications. (b) Plot of aerodynamic resistance to wind velocity in 'Koshihikari' calculated by both the original (r_a', gray dots) and the modified model (r_a, black dots).

Table 2.1. Values and standard errors of leaf area index (LAI) and canopy height (CH) of each genotype, measured on July 15, 2017, with 3 replications.

	Koshihikari	Nipponnbare	Takanari	Habataki	WL	LG	IL23
LAI	3.57 ± 1.04	4.00 ± 1.17	3.95 ± 1.15	3.21 ± 0.96	3.07 ± 0.90	3.60 ± 1.05	3.15 ± 0.91
CH (cm)	85.67 ± 1.18	75.00 ± 1.09	73.00 ± 0.82	74.67 ± 1.42	74.00 ± 1.11	77.33 ± 1.18	70.33 ± 1.14

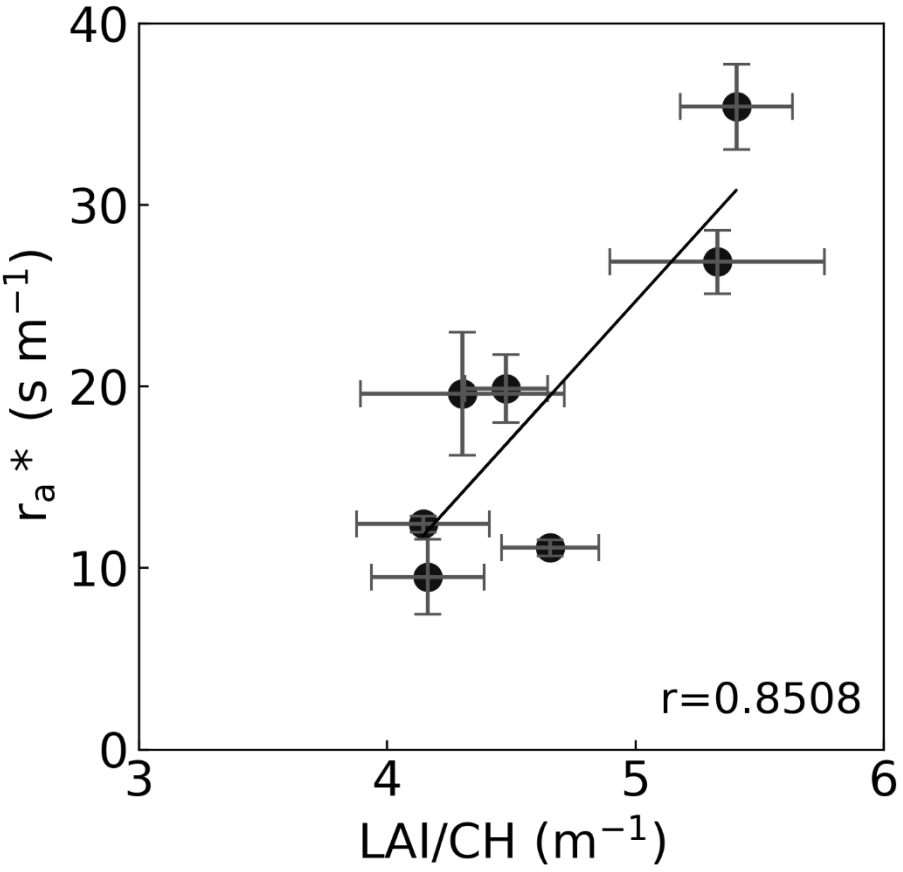

Fig 2.3. The relationship between leaf area density, a ratio of leaf area index to canopy height (LAI/CH), and r_a*. Error bars represent the standard errors.

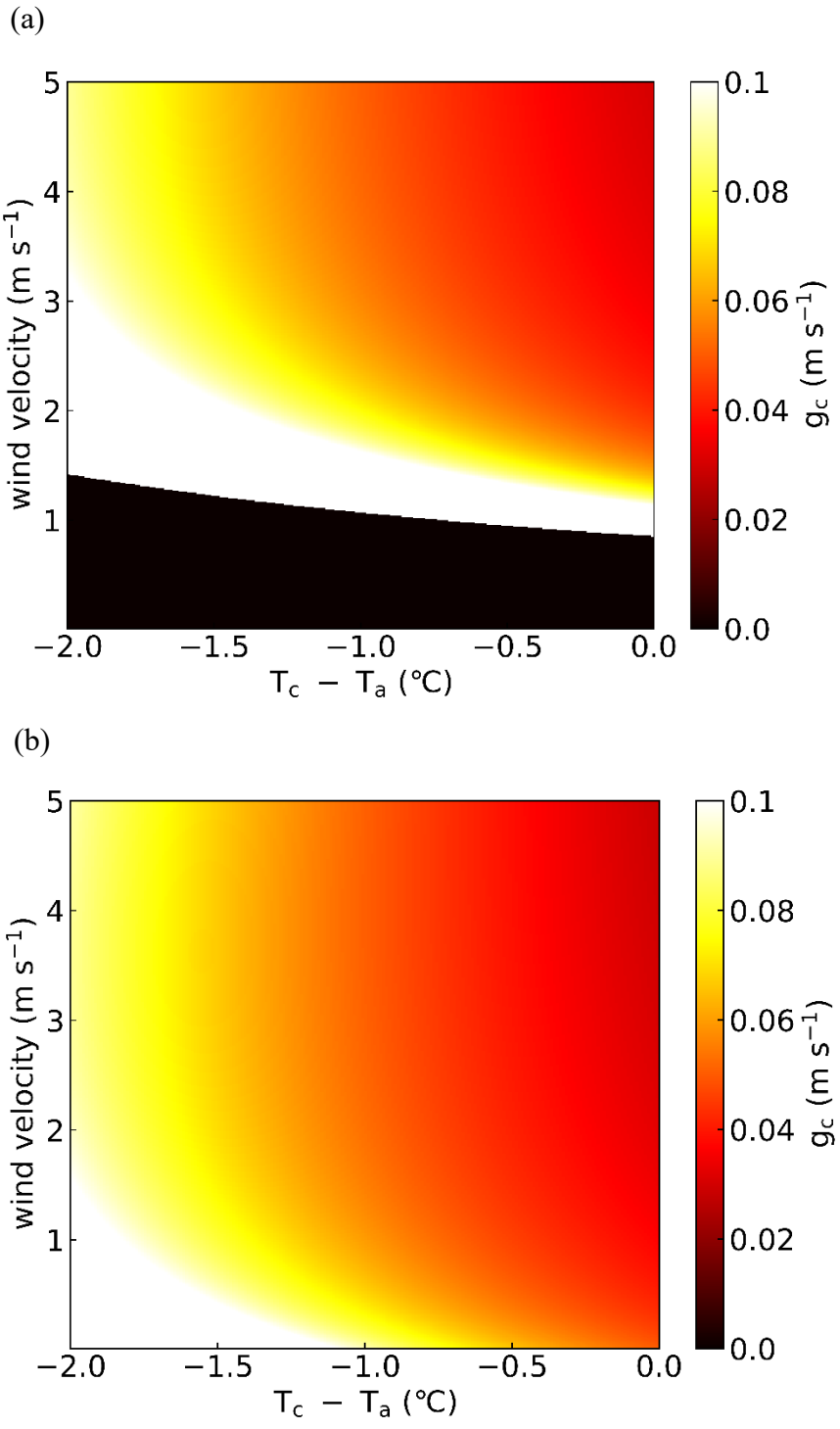

Fig. 2.4. Heatmaps showing canopy diffusive conductance (g_c) estimated by (a) Monteith's original model and (b) our modified model for the combination of canopy temperature depression ($T_c - T_a$) and wind velocity. The weather conditions and plant morphology are set as; T_a = 30 °C, RH = 65 %, R_n = 700 W m^{-2}, plant height = 0.7 m and r_a* = 20 m s^{-1}.

'Takanari', which had the highest r_a* among the seven genotypes, has a larger leaf area, has a larger leaf are and lower plant height (Table 2.1). It is supposed that leaves are dense in these canopies and the gas transfer between the canopy and the atmosphere seems to be relatively difficult in 'Takanari'. Consequently, the resistance of heat transfer from canopies to the atmosphere is suspected to become higher. On the other hand, the cultivars 'Koshihikari', 'Wanlun 422' and 'Liaojing 5' had a lower r_a*. These three cultivars appeared to have canopy structures in which the gas transfer between the canopy and the atmosphere is relatively easy; 'Koshihikari' exhibited larger plant height while 'Wanlun 422' had a smaller leaf area (Table 2.1). Erect panicle type genotypes such as 'Liaojing 5' are reported to have relatively dense leaf distribution in the lower layers of canopies (Hirooka et al., 2018), which may have led to the lower r_a* values recorded.

Because the value of r_a* may be affected by free convection and boundary layer conductance, it can change frequently under field conditions. However, canopy temperature depression in r_a* measurements is approximately 3 °C, which is close to one in the paddy field. Therefore, the value of r_a* in the measurement condition and in the field conditions does not seem to have much difference. Hence the impacts of r_a* change on the r_a in the modified model is considered negligible.

In the original model, r_a diverged from what was expected, especially when wind velocity was under 3.0 m s^{-1}. In particular when wind velocity was lower than 1.0 m s^{-1}, g_c values were sometimes negative. The original model was only applicable to g_c estimation when wind velocity is relatively high. However, such conditions occurred infrequently under field conditions (Fig. 2.5), suggesting that the original model works well in only limited scenarios. By introducing r_a*, the divergence of r_a was successfully avoided even under calm and light air conditions (Fig. 2.2b). This led to the stable

estimation of g_c (see Chapter 3). Our modified model therefore enabled a continuous and stable estimation of canopy gas exchange of rice under field conditions.

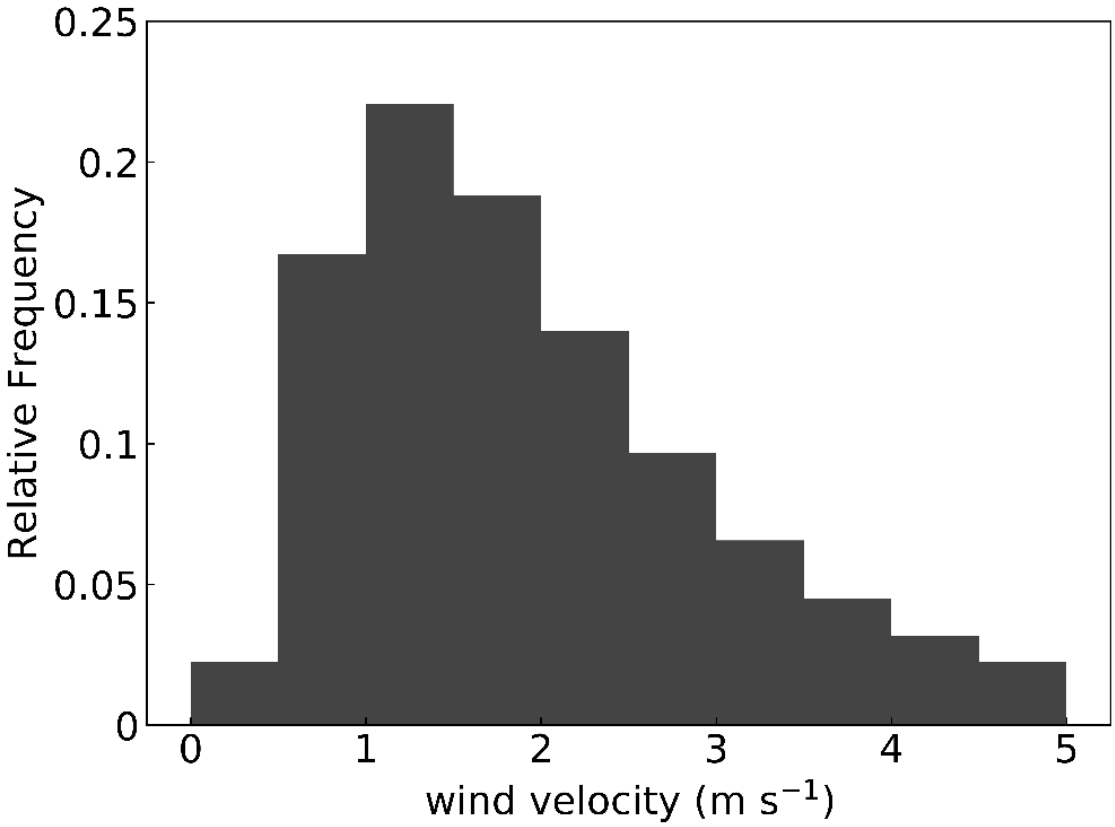

Fig. 2.5. A histogram of wind velocity from July 18 to 25, 2017. Values are normalized.

Chapter 3

Continuous estimation of rice canopy transpiration based on the modified heat balance model

3.1 Introduction

As mentioned in Chapter 1, canopy gas exchange is an important trait for yield formation in the cultivating field in rice. However, to the best knowledge of us, there is little information about diurnal and daily changes of rice canopy transpiration under field conditions. In Chapter 2, the stability of Monteith's heat balance model to the change of wind velocity was improved by the introduction of the concept of r_a*. Thanks to this modification, our newly modified model may be applicable for the continuous estimation of rice canopy transpiration under field conditions.

In this part, we conducted an estimation of rice canopy transpiration with short intervals. The diurnal change of g_c and E, the daily change of cumulative transpiration, and its genotypic difference was evaluated. The relationship between estimated E and final grain yield within 7 rice genotypes was also discussed.

3.2 Materials and Methods

3.2.1 Plant materials and growth analysis

The location of the field and plant materials was same as Chapter 2 (see 2.3.1). Two different types of experimental plots were established for the present study. For yield measurements, a plot of 10 by 13 plants was used with three replications. For canopy temperature measurement, 10 by 10 plants were used with two replications. These two

plots were established in the same field and arranged in a randomized blocked design. The amounts of fertilizer applied as basal-dressing were 60 kg N ha^{-1}, 47 kg P ha^{-1} and 56 kg K ha^{-1}. Weeds, diseases, and insects were strictly controlled, and the field was fully irrigated throughout the entire growing season.

Canopy height was measured for each genotype in the field on July 15, 2017. At the plant maturity stage, 10 plants were chosen, and the grain yield was measured with 3 replications. The grain yield was adjusted to 14% moisture.

3.2.2 Canopy temperature and meteorological data

Canopy surface temperature (T_c) was recorded by infrared thermal imaging camera (InfReC S30, Nippon Avionics Co., ltd., Japan). The camera was set 16 m away from the paddy field and 7 m above the ground level; the angle of elevation was 24º. The resolution of thermal image was 160 × 120 pixels, the spectral range was 8-13 μm, and thermal sensitivity was less than 0.2 °C at 30 °C. The thermal images of each genotype were recorded every second, from July 18 to July 25, 2017. All the plots were covered by the single thermal image and T_c was calculated for each genotype with thermal image processing software NS 9500 (Nippon Avionics Co., ltd.) with two areas in each plot. T_c was corrected using reference temperatures. The temperature reference board was set near the experimental field. White felt was attached on a 60 × 40 cm wooden board. The surface temperature of the reference board was simultaneously recorded by thermometer (TR-52i, T&D Corporation, Japan) and thermal imaging camera. The subtraction of the temperature data on the reference board obtained by these two instruments was used to correct the temperature drift of the thermal imaging camera. It was assumed that canopy surface emissivity was compensated by this temperature correction.

Micro meteorological data at the paddy field was measured using a meteorological data acquisition system. Air temperature and relative humidity was recorded by a temperature and relative humidity probe (CS215, Campbell Scientific, Inc., US) with aspirated radiation shield, wind velocity by an ultrasonic anemometer (1590-PK-020, Gill instruments, Ltd., UK) and upward and downward radiation by an albedo meter (PCR-3, Kipp & Zonen, Netherlands) and infrared radiometer (PRI-01, PREDE CO., Ltd., Japan). Net radiation was calculated as the sum of subtraction of upward and downward radiation of long- and short-wave radiation. These instruments were set approximately 2 m above the ground (1 m above the canopy), connected to a data logger (CR-1000, Campbell Scientific, Inc.) and the values were logged in 1 second intervals, from July 18 to July 25, 2017. Based on these data and the value of r_a* in Chapter 2, g_c and E was estimated.

3.2.3 Statistical analysis

The g_c, E, and yield were represented by the mean value of 4, 4 and 3 replications, respectively. The g_c and E was estimated in two areas in each plot. ANOVA was conducted to compare daily cumulative values of E. A Pearson correlation coefficient was calculated between hourly cumulative E and final grain yield. All these statistical analyses were conducted using R. The calculation of g_c and E was conducted using Python language.

3.3 Results

Typical diurnal changes in R_n and relative humidity (RH) were observed on July 20, 2017 (Fig. 3.1a). The calculated g_c and E in 'Koshihikari' and 'Takanari' showed a similar diurnal pattern to R_n (Fig. 3.1 b and c). The time resolution of the calculation is 1s, and over 99.9% of the total data of g_c ranged from 0 to 0.1 (m s^{-1}), which is similar to that

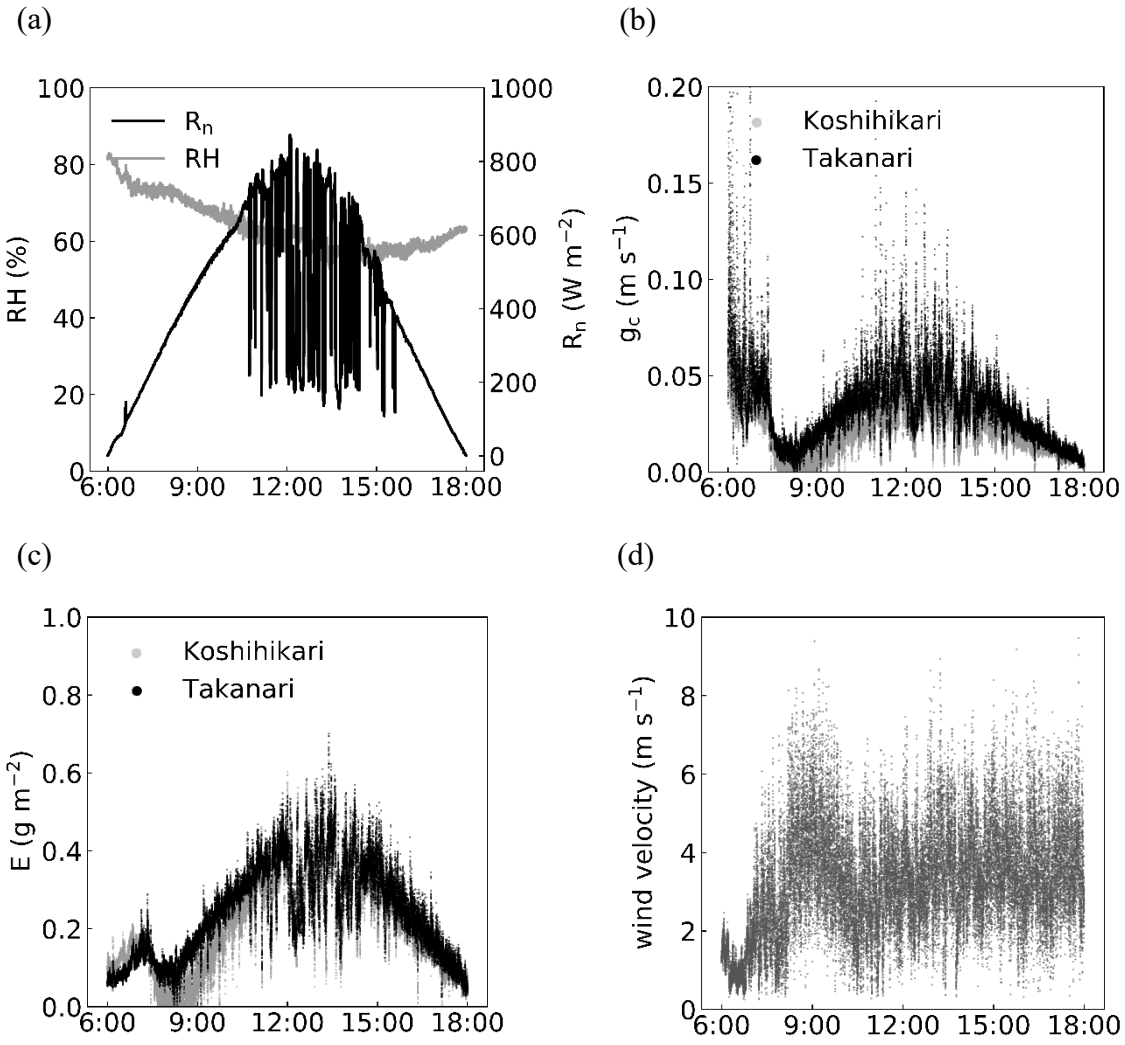

Fig. 3.1. Diurnal changes in (a) net radiation flux density (R_n) and relative humidity (RH), (b) canopy conductance (g_c), (c) canopy transpiration rate (E) and (d) wind velocity on July 20, 2017, in 'Koshihikari' and 'Takanari' calculated by the modified heat balanced model.

found in a previous study for g_c in rice varieties (Horie et al., 2006).

The daily cumulative R_n and cumulative E (kg m^{-2} d^{-1}) of the seven genotypes was calculated from July 18 to 25, 2017 (Fig. 3.2). In all the 7 genotypes, the changes of daily cumulative E corresponded to that of R_n. On July 20, 2017, when cumulative R_n was the highest, cumulative E ranged from 10.29 kg m^{-2} d^{-1} for 'Takanari' to 7.92 kg m^{-2} d^{-1} for 'Nipponbare'. On July 25, cumulative E ranged from 3.26 kg m^{-2} d^{-1} of LG to 2.33 kg m^{-2} d^{-1} of 'IL23'. Significant varietal differences of cumulative E were detected by one-way ANOVA on each day.

The final grain yield ranged from 8.17 t ha^{-1} for 'Takanari' to 5.51 t ha^{-1} for Nipponbare (Table 3.1). Table 3.2 shows the moving correlation coefficients (r) between hourly cumulative E and final grain yield. The r ranged from 0.9664 at 15:00, July 21 to -0.4089 at 17:00, July 25. There were positive correlations between E and grain yield mainly from July 18 to 22, 9:00 to 16:00. After July 23, however, significant correlations were detected in only a few cases.

3.4 Discussion

According to Horie et al. (2006), the range of g_c seems to be reasonable from 0 to 0.1 m s^{-1}. Most of the g_c values estimated by our modified model on July 20 are in this range (Fig. 3.1b), supporting the validity of our model. A clear diurnal pattern of change in g_c and E corresponding to R_n was observed (Fig. 3.1b and c). The g_c and E of 'Takanari' was higher than that of 'Koshihikari', particularly in the mornings. In the morning, g_c showed remarkably high values while R_n was low (Fig. 3.1b). This seems to be due to the morning dews on leaf surface, which leads to the underestimation of the leaf temperature. In Fig 3.1b and c, g_c and E of 'Koshihikari' shows negative values around 8:00. It is

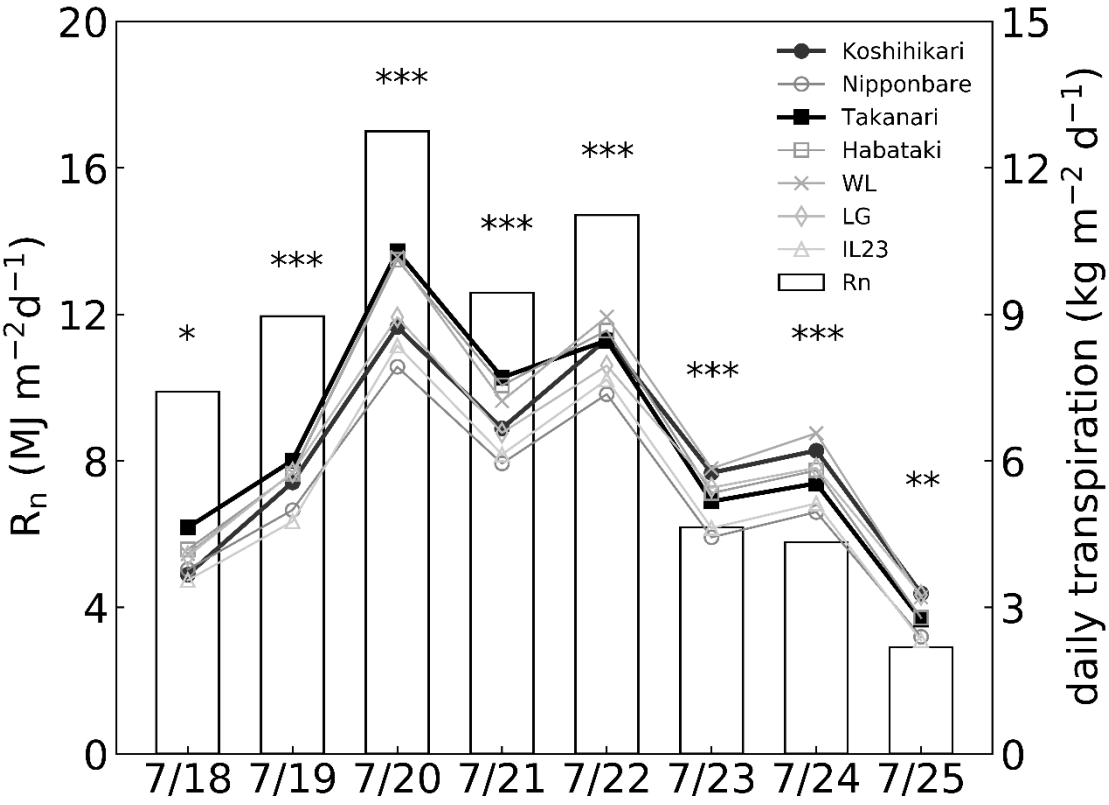

Fig. 3.2. The daily changes of net radiation (R_n) and cumulative transpiration from July 18 to July 25, 2017. The bars represent the R_n, and each line represents the cumulative transpiration in each genotype. The markers *, **, and *** represent the significant genotypic difference with 0.05, 0.01, and 0.001 probability level by one-way analysis of variance (ANOVA), respectively.

Table 3.1. Final grain yield and standard errors (SE) of 7 genotypes. Grain yield was adjusted to 14 % moisture.

	Koshihikari	Nipponbare	Takanari	Habataki	WL	LG	IL23
Yield (t ha^{-1})	6.26	5.51	8.17	7.54	6.20	5.65	5.90
SE	±0.24	±0.13	±0.29	±0.20	±0.15	±0.12	±0.09

Table 3.2. Moving correlation coefficients (r) in hourly intervals between canopy transpiration rate (E) and yield. Significant at 0.05 probability level when $r > 0.7544$ and 0.01 probability level when $r > 0.8746$.

Date	Time											
	0600-	0700-	0800-	0900-	1000-	1100-	1200-	1300-	1400-	1500-	1600-	1700-
18-Jul	0.198	0.090	0.023	0.629	0.793	0.386	0.832	0.736	0.798	0.764	0.310	0.181
19-Jul	-0.193	-0.251	-0.205	0.046	0.794	0.820	0.840	0.650	0.552	0.571	0.864	0.783
20-Jul	-0.183	0.651	0.752	0.751	0.778	0.678	0.524	0.709	0.758	0.895	0.898	0.725
21-Jul	-0.028	-0.008	-0.022	0.772	0.862	0.862	0.848	0.895	0.900	0.966	0.951	0.164
22-Jul	0.317	0.511	0.675	0.689	0.703	0.769	0.577	0.070	0.448	0.335	0.100	-0.355
23-Jul	-0.308	-0.259	-0.258	0.582	0.766	0.590	0.370	0.177	0.268	0.078	-0.025	-0.240
24-Jul	-0.324	-0.355	-0.193	0.156	0.312	0.326	0.313	0.339	0.400	0.458	0.085	-0.318
25-Jul	-0.274	-0.263	-0.211	-0.166	-0.250	0.239	0.469	0.688	0.521	0.465	-0.130	-0.409

thought that the light intensity at leaf surface suddenly increased by the direct irradiation around 8:00, although torn recorded by the sensor steadily increased. Additionally, it is reported that stomatal opening of 'Koshihikari' response to fluctuating light is slower compared to 'Takanari' (Adachi, Tanaka et al., 2019; Taniyoshi et al., 2020). These factors seem cause the jump up of the leaf temperature of 'Koshihikari', which led to the error of g_c and E estimations.

In previous studies, 'Takanari' is reported to have a high photosynthetic capacity (Takai et al., 2010; Takai et al., 2013; Adachi, Yamamoto et al., 2019; Horie et al., 2006). We succeeded in monitoring superior transpiration capacity in 'Takanari' continuously and stably at the canopy level. In addition, we found that the transpiration rate in 'Takanari' decreases in the afternoon, at which point the difference with the transpiration rate of 'Koshihikari' becomes unclear (Fig. 3.1c). Transpiration in 'Takanari' may be limited by water availability under greater vapor pressure deficit conditions. Horie et al. (2006) estimated rice g_c using the thermal imaging and shading method, where varietal differences of g_c were also detected. However, g_c was estimated only under clear weather conditions, and only momentarily (Horie et al., 2006). Hou et al. (2019) estimated the diurnal change of transpiration rate in soybean using thermal imaging in 2 hours intervals. Our study, however, succeeded in estimating rice E in 1 second intervals by introducing the concept of r_a*. Jones et al. (2018) developed a method to estimate g_c and E of cotton canopy in short intervals with a green hemispherical reference, but they did not examine any genotypic differences. Using our method, Monteith's original model can be modified based on the direct measurement of r_a* in each genotype. To our knowledge, this study is the first one which has enabled high-resolution, continuous and stable estimation of rice canopy diffusive conductance and transpiration rate, and the detection of the genotypic

difference of E under field conditions.

Based on the modified model, daily cumulative E in each genotype was calculated. Daily cumulative E changed depending on the value of R_n. Varietal differences of daily cumulative E were detected on each day (Fig. 3.2). Throughout the measurement period, daily cumulative E was consistently higher in 'Takanari', WL and 'Habataki', and consistently lower in 'Koshihikari', 'Nipponbare' and 'IL23', regardless of the value of daily cumulative R_n. This tendency coincides with photosynthetic capacity reported in previous studies (Takai et al., 2010; Hirasawa et al., 2010), which supports the validity of the model.

It is reported that 60 days after transplanting, daily cumulative E ranges from 2 to 10 kg m^{-2} d^{-1} with a micro lysimeter measurement (Adachi et al., 1995; Yan & Oue, 2011), which is comparable to the daily cumulative E estimated by the modified model in our study. This match also supports the validity of our model. Significant correlations between hourly cumulative E and final grain yields were detected, mainly from July 18 to 21, 9:00 to 16:00 (Table 3.2). In particular, the 'Takanari', 'Habataki', and WL varieties had consistently higher transpiration rates and final grain yields (Fig. 3.2 and Table 3.1). This implies that E in the daytime before the heading stage is important for yield formation in rice. This corresponds to a previous study which reported a significant correlation between g_c estimated under clear weather conditions and final grain yield (Horie et al., 2006). However, after July 22, this relationship broke down. It is thought that E values seemed nearly maximum under clear weather condition before July 22, which led to the high correlation with final grain yield, while the difference of E in 7 genotypes rarely was observed after July 23 because of the low radiation. The relationship between photosynthetic capacity and grain yield has been well discussed in rice (Shimono

et al., 2009; Chang et al., 2016; Luo et al., 2020). The positive relationships observed in the present study support the validity of *E* estimated by our method.

Chapter 4

Prediction of rice canopy transpiration rate by neural networks and an evaluation of its response to various meteorological conditions

4.1 Introduction

In Chapter 2, a method for estimating rice canopy transpiration with high stability and time-resolution was developed, and its applicability under field conditions was shown in Chapter 3. However, this technique still requires many labor costs for its utilization, mainly in measurements of T_c and r_a*. Besides, the fluctuation of the estimated values cannot be negligible because the heat balance theory stands on the steady state, while canopies of field-grown rice are under non-steady environments.

To estimate E, meteorological data are also required in many cases. Unlike canopy surface and reference temperatures, meteorological data are relatively easy to access. After setting up the weather station, the meteorological data are recorded automatically. Micrometeorological conditions strongly affect canopy transpiration (Jones, 2014). For instance, favorable temperature and strong radiation accelerate photosynthesis in general (Choudhury, 1987; Yamori & Hikosaka, 2014), which leads to stomatal opening and greater transpiration. Further, air humidity affects stomatal aperture and transpiration rate (Morison & Gifford, 1983; Monteith, 1995). Under field conditions, however, meteorological factors changing with high complexity, which makes it difficult to explain relationships between meteorological conditions and canopy gas exchange clearly.

Neural network is a mathematical model in which the structure of human brain is imitated and a powerful tool to explain non-linear relationships. Recently, many studies

have been conducted to utilize neural networks in the field of plant science. For instance, neural networks have been used for the prediction of biomass (Ma et al., 2019; Jin et al., 2020), final yield (Das et al., 2020; Haghverdi et al., 2018; Nevavuori et al., 2019), transpiration (Nam et al., 2019; Fan et al., 2021), and detection of crop diseases (Mujahidin et al., 2021) in previous studies. A study to substitute a process-based model for the prediction of rice grain yield using a neural network has also been conducted (Yamamoto, 2019). However, to the best of our knowledge, no studies have been conducted to apply the neural network for predicting *E* in rice under field conditions. In general, numerous datasets are required for training and establishing an accurate model using a neural network. We developed a method to estimate *E* in rice under field conditions with a high time resolution, as mentioned above. This technique enabled the acquisition of a large-scale dataset of meteorological conditions and *E* in two cultivars with different gas exchange characteristics, 'Koshihikari' and 'Takanari'. Therefore, the numerous datasets of these two factors in 'Koshihikari' and 'Takanari' may be applied to establish a model to predict *E* based on meteorological data, without the measurement of canopy surface temperature and the settings of some references.

Sensitivity analysis is a technique to be used to evaluate the contribution of each parameter to the output of the model (Hamby, 1994). The response of the predicted value of *E* to the change in the input meteorological data can be tested by sensitivity analysis. To date, the gas exchange activity and genotypic differences in rice under steady or simple environmental conditions have been reported in many studies (Qu et al., 2016; Ikawa et al., 2017; Yamori et al., 2020). Many previous studies have reported that the saturated photosynthetic rate in a single leaf was greater in 'Takanari' than in *japonica* cultivars, including 'Koshihikari' (Hirasawa et al., 2010; Adachi, Yamamoto et al., 2019; Takai et

al., 2010; Taylaran et al., 2011). However, little information has been published regarding gas exchange and its genotypic differences under various combinations of meteorological conditions. Acquiring this information is important to gain a better understanding of gas exchange, growth processes, and genotypic differences under field conditions in rice.

By introducing neural network and sensitivity analysis, a part of *E* estimation process, canopy-related parameters and heat balance equations, can be substituted by a neural network structure. It is thought that this substitution enables to cancel the fluctuation of *E* unique to the heat balance equations, and to connect meteorological data and *E* directly. This means that feature extractions of the response of canopy gas exchange to the change of meteorological conditions may be possible and that its genotypic differences can be evaluated.

In the present study, we first developed a model to predict *E* using micrometeorological data and a neural network. The *E* values under various meteorological conditions were simulated using sensitivity analysis. Based on the results of this analysis, the genotypic difference in the response of predicted *E* to the meteorological conditions between 'Koshihikari' and 'Takanari' was evaluated.

4.2 Materials and Methods

4.2.1 Plant materials

In 2017, 2018, and 2019, 'Koshihikari' and 'Takanari' were cultivated in paddy fields at the Graduate School of Agriculture, Kyoto University, Kyoto, Japan (35° 2′ N, 135° 47′ E, 65 m altitude). The seeds were sown on April 20, 2017, April 23, 2018, and April 19, 2019, and the seedlings were transplanted on May 16, 2017, May 18, 2018, and May 17, 2019, respectively. The planting density was 22.2 plants·m^{-2}. The amount of

fertilizer applied as basal dressing was 60 kg $N \cdot ha^{-1}$, 47 kg $P \cdot ha^{-1}$, and 56 kg $K \cdot ha^{-1}$ in all three years. In 2018 and 2019, 40 kg $N \cdot ha^{-1}$, 31 kg $P \cdot ha^{-1}$, and 37 kg $K \cdot ha^{-1}$ were additionally applied as top-dressing at the beginning of July. Weeds, diseases, and insects were strictly controlled, and the field was fully irrigated throughout the growing season.

4.2.2 Estimation of E by the heat balance model

Micrometeorological data at the paddy field were measured using a meteorological data acquisition system from July 18 to 25 over three years. In 2017, micrometeorological data were recorded using the method described in Chapter 2 and 3. In 2018 and 2019, air temperature (T_a), relative humidity (RH), and wind velocity were recorded using a composite meteorological sensor (WS500, EKO Instruments, Japan). Solar radiation was recorded using a pyranometer (MS802, EKO Instruments, Japan). In 2018, the upward and downward radiation was collected using an albedo meter (PCR-3, Kipp & Zonen, Netherlands) and infrared radiometer (PRI-01, PREDE CO., Ltd., Japan). All sensors were connected to a data logger (GL840, GRAPHTEC Co., Japan). The net radiation (R_n) in 2017 and 2018 was calculated as the sum when the upward and downward radiation of long- and short-wave radiations are subtracted. The R_n in 2019 was estimated based on the relationship between solar radiation and net radiation recorded from July 10 to 25, 2018 (Fig. 4.1). In all three years, the canopy surface temperature was recorded using the method described in Chapter 3, and the value of r_a* was represented by the value shown in Chapter 2. Canopy height was recorded before and after the estimation period, and canopy height on each day was estimated under the assumption that canopy height increased linearly during this period. From these data, E was estimated from 6:00:00 to 18:00:00 in 1-second intervals.

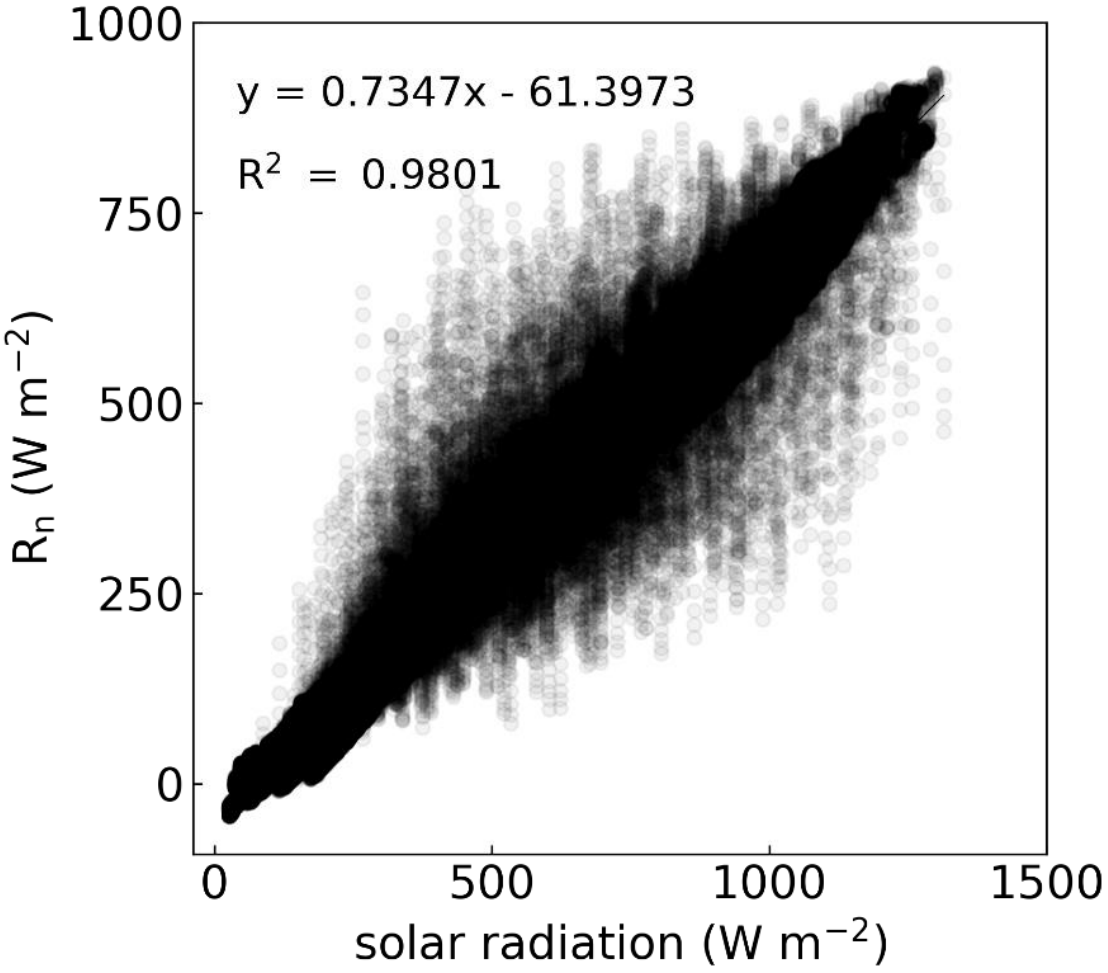

Fig. 4.1. The relationship between solar radiation and net radiation based (R_n) on the micrometeorological data acquired from July 10 to 25, 2018.

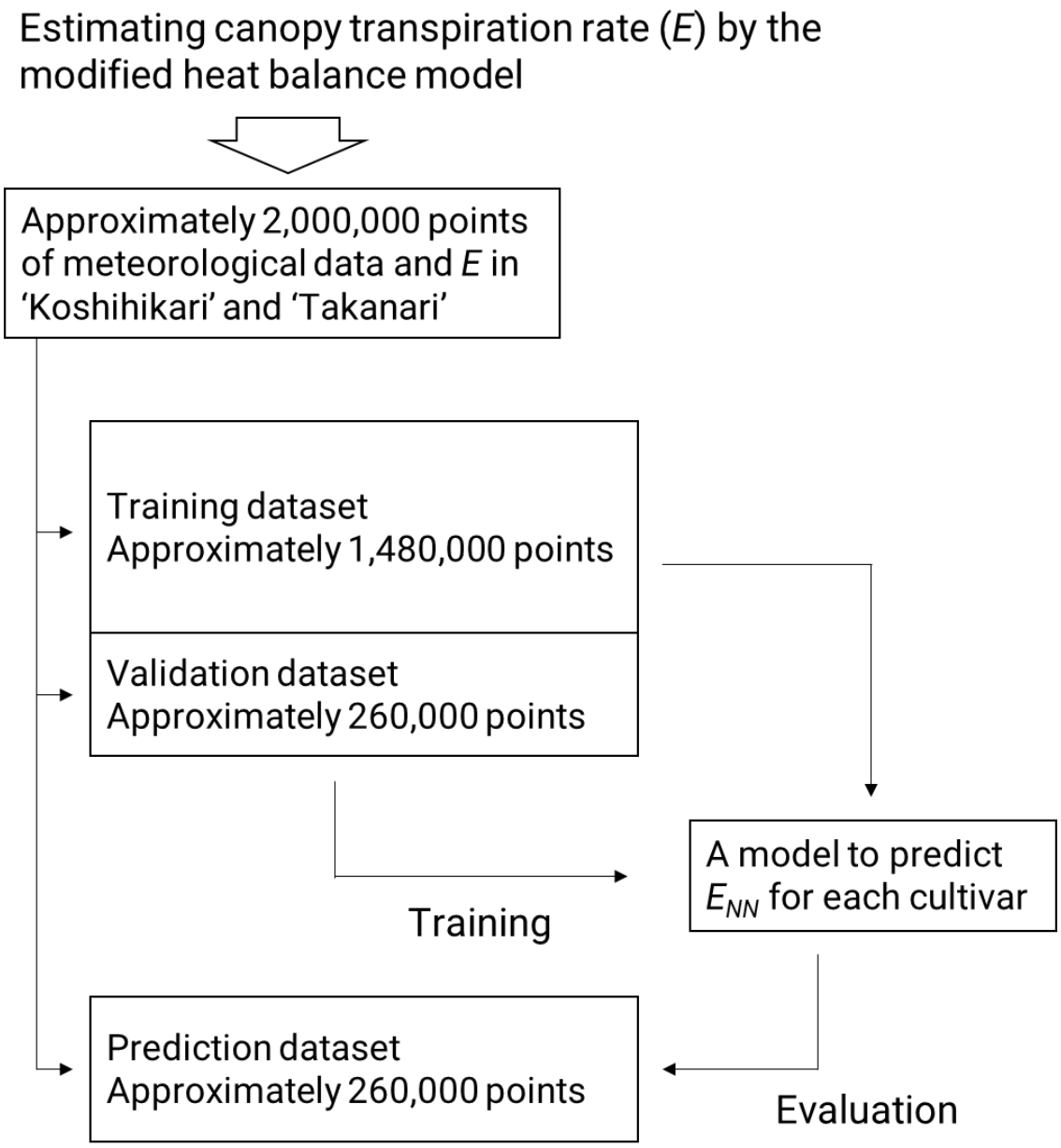

Fig. 4.2. Schematic of the process used to predict canopy transpiration rate in 'Koshihikari' and 'Takanari' by the neural networks.

4.2.3 Dataset, model establishment, and prediction

A schematic of this process is displayed in Fig. 4.2. Data on meteorological conditions and E from July 18 to 25 in 2017, 2018, and 2019 were used. The meteorological data included time, T_a, RH, and R_n. All parameters were normalized, ranging from 0 (representing 6:00:00) to 1 (representing 18:00:00) for time, 0 (representing 20 °C) to 1 (representing 40 °C) for T_a, 0 (representing 0%) to 1 (representing 100%) for RH, and 0 (representing -50 W m^{-2}) to 1 (representing 1450 W m^{-2}) for R_n. The real value acquired using the method described above was used for E. After this preprocessing, the datasets, except those collected on July 22, 2017, July 21, 2018, and July 24, 2019, were used for model establishment. The model was established using a PC-based deep learning tool (Neural Network Console, Sony Co., Japan). The input variables were time, T_a, RH, and R_n, while the output variables were E. The model structure was determined by an automatic optimization method, 'Structure Search', included in the Neural Network Console. The model structure was established based on the 'Koshihikari' dataset. Based on the established model structure, E on July 22, 2017, July 21, 2018, and July 24, 2019, was predicted for 'Koshihikari' and 'Takanari', respectively. In the prediction, training and validation were independently conducted for the two cultivars. The predicted value of E is called E_{NN}.

4.2.4 Analysis

After the prediction, diurnal change patterns of E and E_{NN} were compared, and the coefficient of determination (R^2) and root mean squared error (RMSE) were calculated. The E_{NN} under virtual meteorological conditions was simulated based on the established model. In the simulation datasets, two of the four input variables were sequentially

changed, and the other two variables were fixed in three patterns (Table 4.1). From these datasets, E_{NN} under virtual meteorological conditions was predicted for 'Koshihikari' and 'Takanari'. After the prediction, the simulated E_{NN} values for the two cultivars were compared. All calculations and analyses were conducted in the Python language.

4.3 Results

4.3.1 Meteorological condition

The daytime mean T_a, mean RH, and cumulative R_n from July 18 to 25 in 2017, 2018, and 2019 are shown in Fig. 4.3. The mean T_a ranged from 25.43 °C on July 19, 2019, to 33.48 °C on July 18, 2018. The mean RH ranged from 53.21% on July 24, 2018, to 93.55% on July 22, 2019. The cumulative R_n ranged from 1.90 $MJ \cdot m^{-2} \cdot d^{-1}$ on July 22, 2019, to 17.97 $MJ \cdot m^{-2} \cdot d^{-1}$ on July 24, 2018. Generally, the meteorological conditions in 2018 were hot and dry, while in 2019, it was cool and humid. The year 2017 had various weather conditions: hot and dry, cool and humid, and an intermediate condition.

4.3.2 Prediction of E by neural network

The structure of the established model is illustrated in Fig. 4.4. The E_{NN} values were well predicted using neural networks on July 22, 2017, and July 21, 2018, for both 'Koshihikari' (R^2 = 0.7598, RMSE = 0.0597 in 2017 and R^2 = 0.8079, RMSE = 0.0752, in 2018; Fig. 4.5) and 'Takanari' (R^2 = 0.8537, RMSE = 0.0392, in 2017 and R^2 = 0.8431, RMSE = 0.0538 in 2018, Fig. 4.5). However, the E_{NN} value on July 24, 2019, did not work well for 'Koshihikari' (R^2 = 0.2003, RMSE = 0.0967, Fig. 4.5). The E_{NN} of 'Takanari' on July 24, 2019, was better predicted than that of 'Koshihikari', but not in 2017 and 2018 (R^2 = 0.7147, RMSE = 0.0554, Fig. 4.5).

Table 4.1. The fixed and sequenced values of the input variables.

Variables	Fixed value	Sequenced value
Time	9:00 (0.375), 12:00 (0.5), 15:00 (0.625)	6:00 ~ 18:00 (0.25 ~ 0.75)
Air temperature (T_a, °C)	25 (0.25), 30 (0.5), 35 (0.75)	20 ~ 40 (0 ~ 1)
Relative humidity (RH, %)	40 (0.4), 65 (0.65), 90 (0.9)	30 ~ 100 (0.3 ~ 1)
Net radiation (R_n, W m^{-2})	150 (0.133), 450 (0.333), 750 (0.533)	-50 ~ 1075 (0 ~ 0.75)

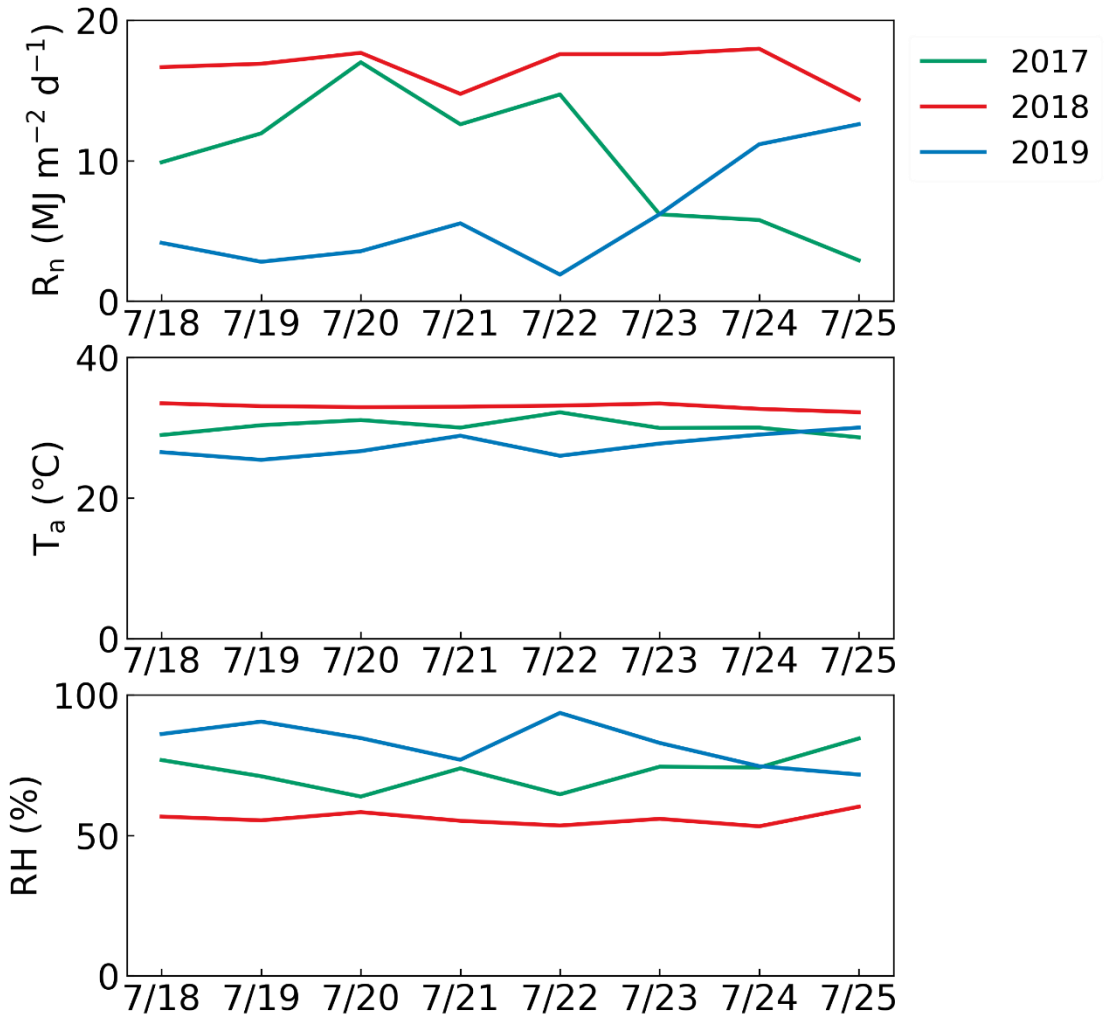

Fig. 4.3. Daily cumulative net radiation (R_n, top), mean air temperature (T_a, middle), relative humidity of the air (RH, bottom) from July 18 to 25 in 2017, 2018, and 2019. The green, red, and blue lines represent the values in 2017, 2018, and 2019, respectively.

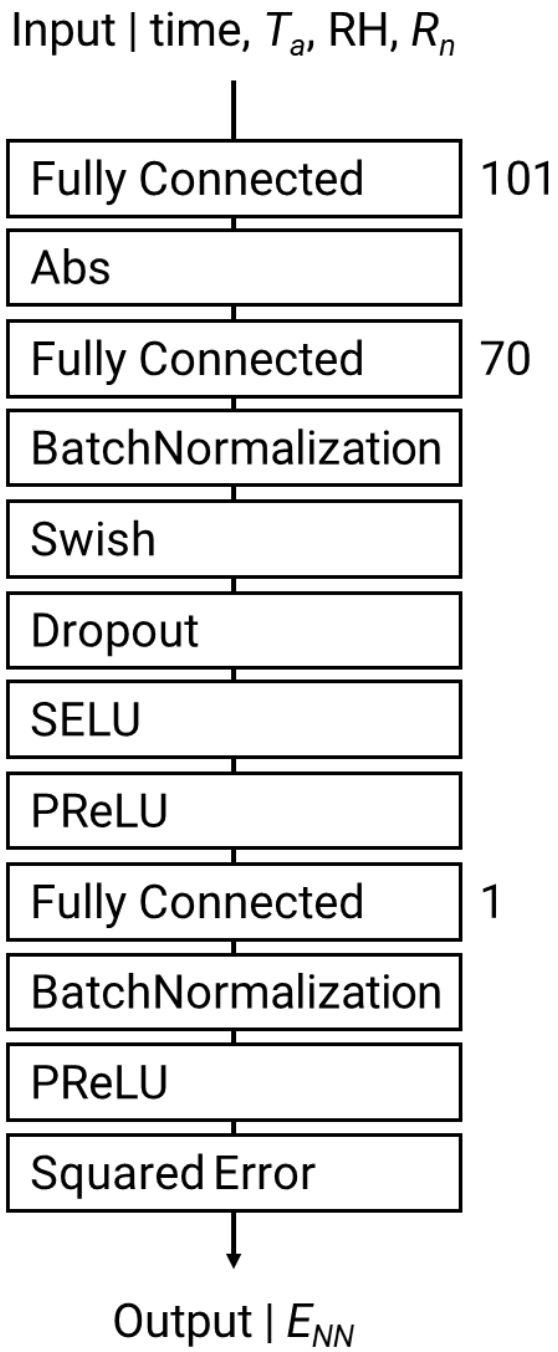

Fig. 4.4. The structure of the model for predicting canopy transpiration rate. Each component can be explained by: Fully connected, Fully Connected Layer; Abs, Absolute Value; Dropout, Dropout Layer; SELU, Scaled Exponential Linear Unit; PReLU, Parametric Reflected Linear Unit; and SquaredError, Output Layer minimizing the squared error. The numbers next to the Fully Connected Layers represent the size of outshapes.

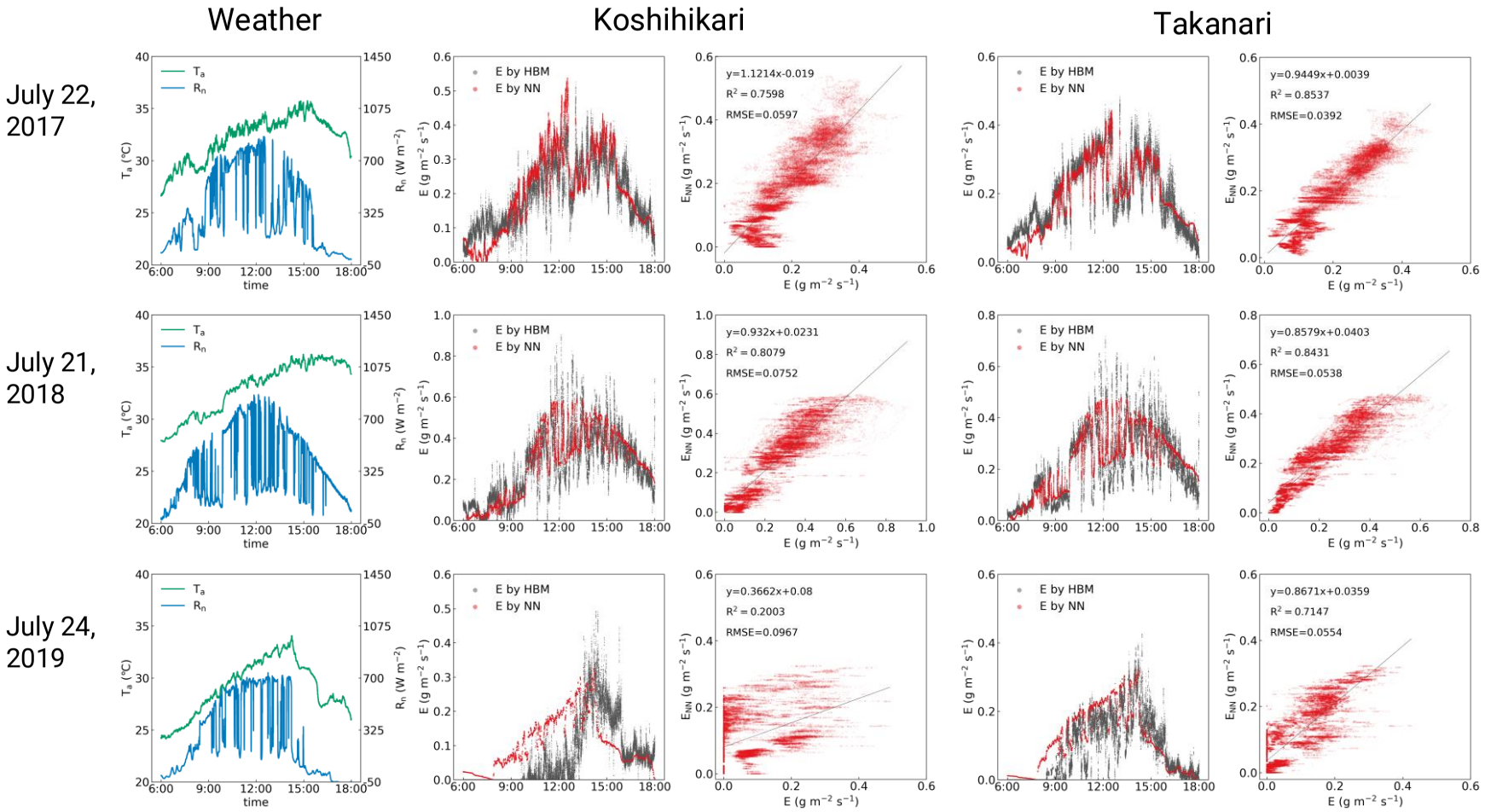

Fig. 4.5. Weather conditions and results of the *E* prediction in 'Koshihikari' and 'Takanari' on July 22, 2017, July 21, 2018, and July 24, 2019. For each cultivar, left panels show the diurnal change in *E* estimated by the heat balance model (*E* by HBM, black dots) and E_{NN} predicted by the model based on the neural network (*E* by NN, red dots). Right panels show the relationship between *E* and E_{NN}.

Figure 4.6 shows the scatterplots of time and RH in three years for the measured E in the separated nine panels for, T_a under 26.6, from 26.6 to 33.3, or over 33.3 ℃ and R_n under 300, from 300 to 600, or over 600 W m^{-2}. The colors of the datasets represent the ratio of E in 'Takanari' (E_{Taka}) to 'Koshihikari' (E_{Koshi}) based on the values estimated by the heat balance model. Of the datasets, 61.15% were included in the R_n panels under 300 W m^{-2} (panels a, b, and c). A total of 15.12% of the datasets were included in the panel of T_a under 26.6 °C and R_n under 300 W m^{-2} (panel a), and most were plotted on the area of RH over 75% from 6:00 to 18:00. In panel a, E in 'Takanari' was higher than that in 'Koshihikari', mainly from 9:00 to 10:30, but lower at the other timepoint. A total of 39.32% of the datasets were included in the panel of T_a from 26.6 to 33.3 ℃ and R_n under 300 W m^{-2} (panel b), and most were plotted on the area of RH over 50% from 6:00 to 18:00. In panel b, E in 'Takanari' was higher than that in 'Koshihikari', mainly from 9:00 to 15:00, and lower at the other timepoint. A total of 6.71% of the datasets were included in the panel of T_a from over 33.3 °C and R_n under 300 W m^{-2} (panel c), and most were plotted on the area of RH approximately under 65% from 12:00 to 18:00. In panel c, E in 'Takanari' was generally lower than that in 'Koshihikari'. Most of the other datasets were included in four panels: the panels of R_n from 300 to 600 W m^{-2} or over 600 W m^{-2} and T_a from 26.6 °C to 33.3 °C or over 33.3 °C (panels e, f, h, and i). A total of 14.27% of the datasets were included in the panel of T_a from 26.6 °C to 33.3 °C and R_n from 300 to 600 W m^{-2} (panel e), and most were plotted on the area of RH over 50% from 7:00 to 17:00. In panel e, E in 'Takanari' was generally higher than that in 'Koshihikari'. A total of 6.67% of the datasets were included in the panel of T_a over 33.3 °C and R_n from 300 to 600 W m^{-2} (panel f), and most were plotted on the area of RH approximately under

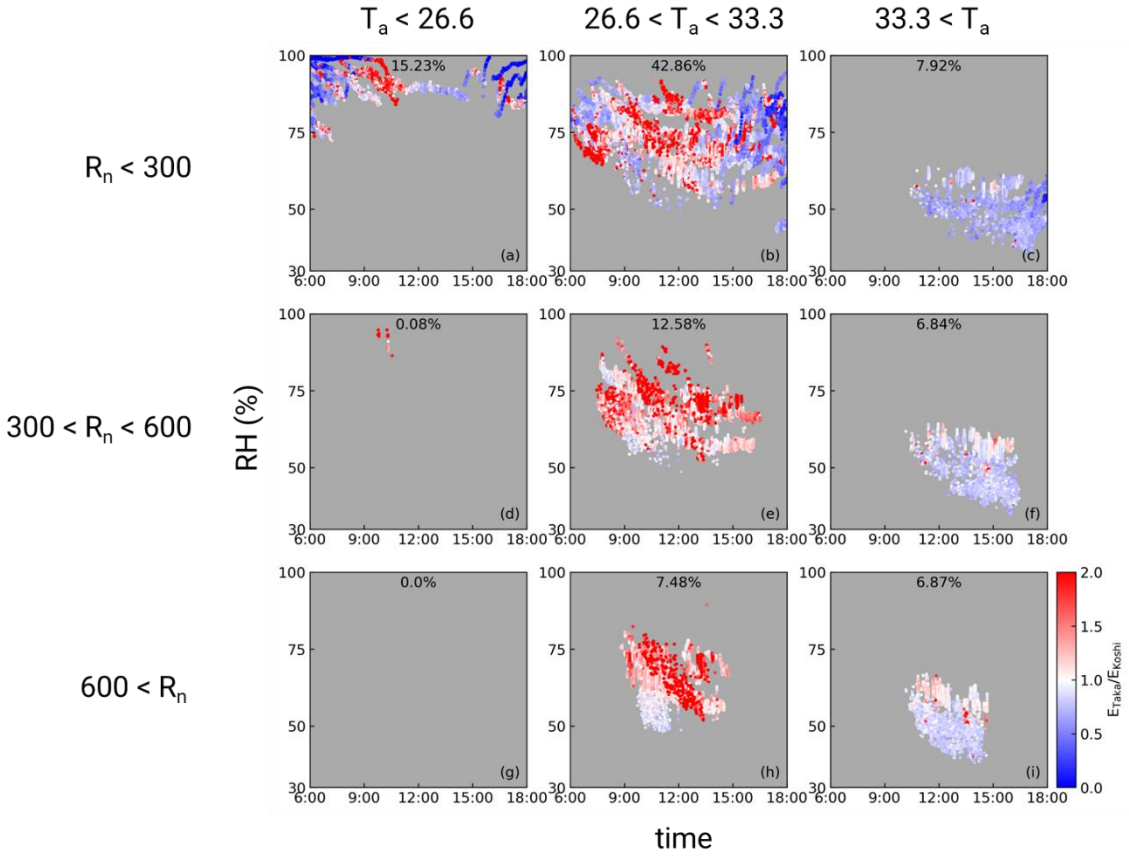

Fig. 4.6. The scatterplots of meteorological data and varietal difference in the canopy transpiration rate between 'Koshihikari' and 'Takanari' over 3 years. The time and relative humidity (RH) are presented on the x and y axis, respectively. The color of the data points represents the ratio of *E* in 'Takanari' to 'Koshihikari' estimated by the heat balance model. All data for the scatterplots of time and RH over 3 years were separated into 9 groups: T_a under 26.6, from 26.6 to 33.3, and over 33.3 ℃ x R_n under 300, from 300 to 600, and over 600 W·m^{-2}.

65% from 10:00 to 17:00. In panel f, E in 'Takanari' was generally lower than that in 'Koshihikari'. A total of 9.33% of the datasets were included in the panel of T_a from 26.6 to 33.3 ℃ and R_n over 600 W m^{-2} (panel h), and most were plotted on the area of RH from 50 to 75% from 9:00 to 15:00. In panel h, E in 'Takanari' was generally higher than that in 'Koshihikari'. A total of 8.25% of the datasets were included in the panel of T_a over 33.3 °C and R_n over 600 W m^{-2} (panel i), and most were plotted on the area of RH under 65% from 10:00 to 15:00. In panel i, E in 'Takanari' was generally lower than that in 'Koshihikari'. In the other plots, only a few datasets were included in the panel of T_a under 26.6 ℃ and R_n from 300 to 600 W m^{-2} (panel d), and no datasets were included in the panel of T_a under 26.6 ℃ and R_n over 600 W m^{-2} (panel g).

Figure 4.7 shows the scatterplots by T_a and R_n over three years for the measured E in the separated nine panels for, the time before 10:00, from 10:00 to 14:00, or after 14:00 °C and RH under 52.5%, from 52.5% to 77.5%, or over 77.5 %. The colors of the datasets represent the ratio of E in 'Takanari' to 'Koshihikari' based on the values estimated by the heat balance model. The datasets were included in all panels, except panel a: the time before 10:00 and RH under 52.5%. A total of 6.62% of the datasets were included in the panel for time from 10:00 to 14:00 and RH under 52.5% (panel b), and most were plotted on the area of T_a around 35 °C and R_n under 900 W m^{-2}. In panel b, E in 'Takanari' was generally lower than that in 'Koshihikari'. Of the datasets, 10.19% were included in the panel of time after 14:00 and RH under 52.5% (panel c), and most were plotted on the area of T_a around 35 °C and R_n under 700 W m^{-2}. In panel c, E in 'Takanari' was generally lower than that in 'Koshihikari'. A total of 14.23% of the datasets were included in the panel for time before 10:00 and RH from 52.5% to 77.5% (panel d), and

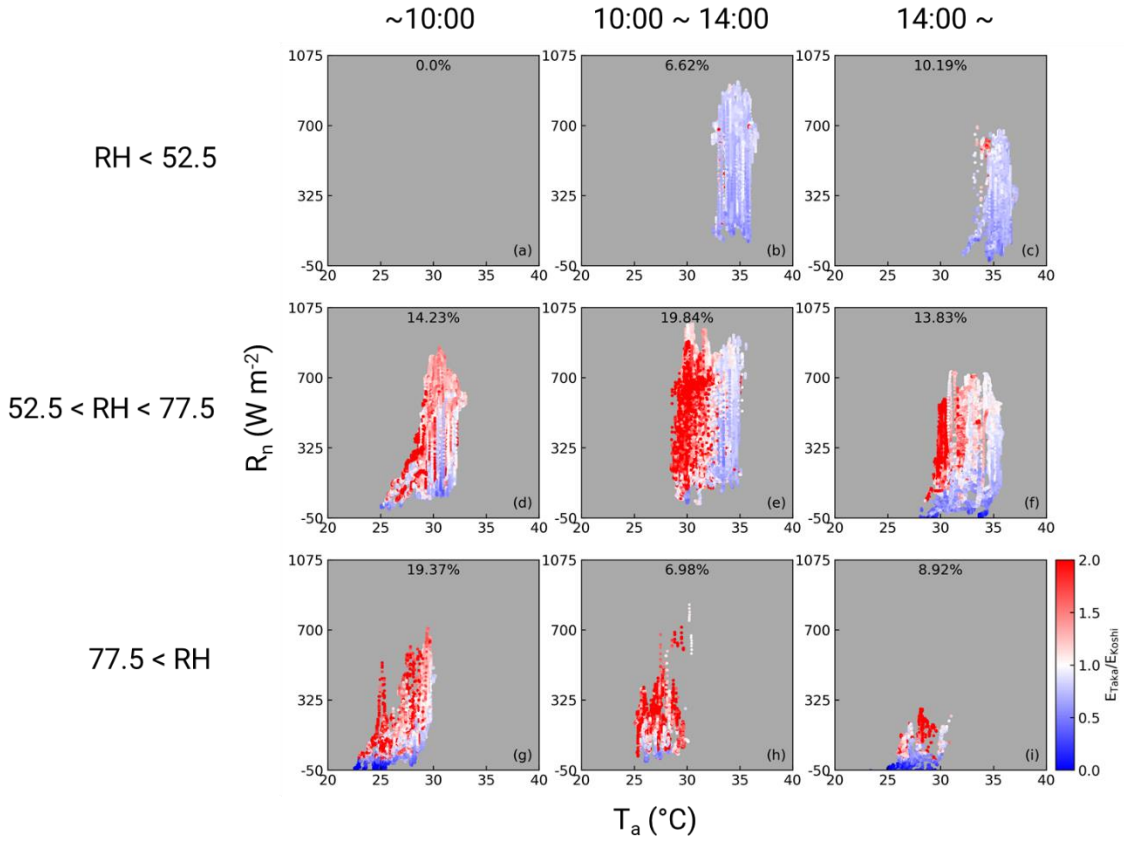

Fig. 4.7. Scatterplots of meteorological data and varietal difference in the canopy transpiration rate between 'Koshihikari' and 'Takanari' over 3 years. Air temperature (T_a) and net radiation (R_n) are presented on the x and y axis, respectively. The color of the data points represents the ratio of E in 'Takanari' to 'Koshihikari' estimated by the heat balance model. All data were separated into 9 groups: the time before 10:00, from 10:00 to 14:00, and after 14:00 x RH under 52.5%, from 52.5 to 77.5%, and over 77.5%. The value above represents the percentage of included data relative to all meteorological data.

most were plotted on the area of T_a from 25 to 33 °C and R_n under 700 W m^{-2}. In panel d, E in 'Takanari' was lower than that in 'Koshihikari' mainly under two conditions: when T_a was around 30 °C and R_n was weaker than 700 W m^{-2}, and when T_a was around 25 °C. Of the datasets, 19.84% were included in the panel for time from 10:00 to 14:00 and RH from 52.5% to 77.5 % (panel e), and most were plotted on the area of T_a from 28 to 33 °C and R_n under 900 W m^{-2}. In panel e, E in 'Takanari' was generally higher than that in 'Koshihikari' when T_a was lower than 32 °C, but lower when T_a was higher than 32 °C. Of the datasets, 13.83% were included in the panel for time after 14:00 and RH from 52.5% to 77.5% (panel f), and most were plotted on the area of T_a from 30 to 35 °C and R_n under 700 W m^{-2}. In panel f, E in 'Takanari' was generally higher than that in 'Koshihikari' when R_n was stronger than 300 W m^{-2} and T_a was lower than 33 °C. A total of 19.37% of the datasets were included in the panel for time before 10:00 and RH over 77.5% (panel g), and most were plotted on the area of T_a under 30 °C and R_n under 700 W m^{-2}. In panel g, E in 'Takanari' was generally higher than that in 'Koshihikari' when R_n was over 100 W m^{-2}. Of the datasets, 6.98% were included in the panel of time from 10:00 to 14:00 and RH over 77.5% (panel h), and most were plotted on the area of T_a from 25 to 30 °C and R_n under 400 W m^{-2}. In panel h, E in 'Takanari' was generally higher than that in 'Koshihikari'. Of the datasets, 8.92% were included in the panel of time from after 14:00 and RH over 77.5% (panel i), and most were plotted on the area of T_a from 25 to 30 °C and R_n under 300 W m^{-2}. In panel i, E in 'Takanari' was generally higher than in 'Koshihikari' when R_n was over 100 W m^{-2}.

The ratio of the simulated E_{NN} in 'Takanari' to 'Koshihikari' under various meteorological conditions is shown in Figs. 4.8 and 4.9. The settings of the meteorological conditions in Figs. 4.8 and 4.9 were same with the classifications of Figs.

4.6 and 4.7, respectively. These two heatmaps were drawn only in the part where the meteorological data were observed in Figs. 4.6 and 4.7. In Fig. 4.8, time and RH ranged from 6:00 to 18:00 and 30 to 100 %, respectively. The other two input variables, T_a and R_n, were fixed at 25, 30, or 35 °C, and 150, 450, and 750 W m^{-2}, respectively. These nine panel patterns are shown. When T_a was fixed at 25 ℃, the E_{NN} of 'Takanari' was superior to that of 'Koshihikari' mainly from 9:00 to 15:00 and RH under 90% (panel a). When T_a was fixed at 30 °C, the E_{NN} in 'Takanari' was superior to that in 'Koshihikari', mainly from 50% to 75% RH (panels b, e, and h). However, when T_a was fixed at 35 °C, the E_{NN} in 'Takanari' was generally lower than that in 'Koshihikari' (panels c, f, and i). In Fig. 4.9, T_a and R_n ranged from 20 to 40 °C and -50 to 1075 W m^{-2}, respectively. The other two input variables, time and RH, were fixed at 9:00, 12:00, and 15:00, and 40, 65, or 90%, respectively. These nine panel patterns are shown. The E_{NN} in 'Takanari' was superior to that in 'Koshihikari', mainly under the conditions of T_a from 25 to 30 °C and R_n under 1000 W m^{-2}.

4.4 Discussion

The E_{NN} values were found to fit the values of E estimated based on the modified heat balance model in 2017 and 2018, but not in 2019, especially in 'Koshihikari' (Fig. 4.5). On July 24, 2019, T_a was remarkably low. As a result, RH was high compared to the other two days. However, the value of R_n was as large as that of the other two days. Under such situations, the stomatal conductance in 'Koshihikari' was low, and the estimation of canopy transpiration rate based on the heat balance model became unstable, leading to unexpected values on July 24 (black points in Fig. 4.5). Therefore, improvement is necessary for the heat balance model under such meteorological conditions.

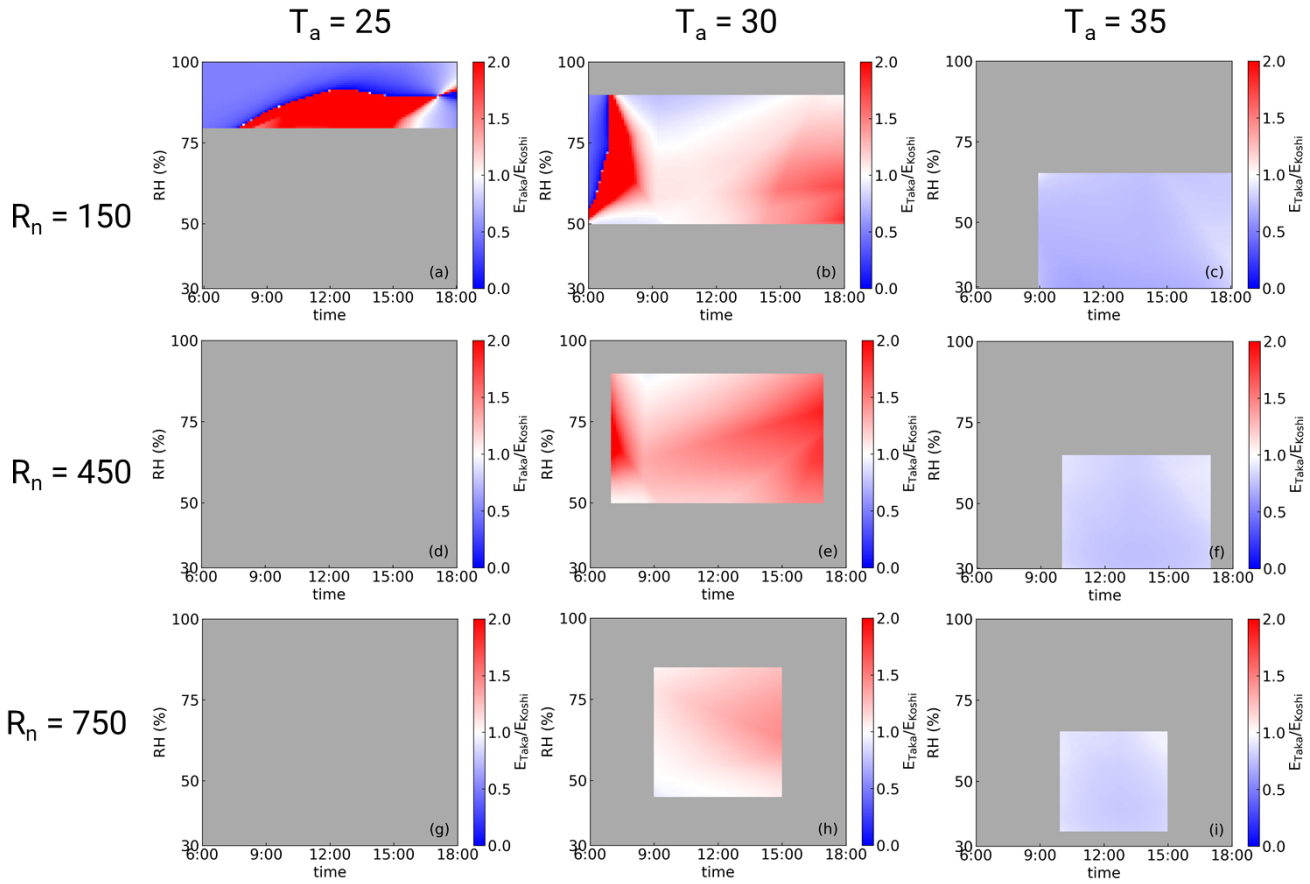

Fig. 4.8. Heatmap showing the varietal difference in the simulated values of canopy transpiration rate (E_{NN}) in 'Koshihikari' and 'Takanari'. Red, white, and blue represent the ratio of the simulated value of E_{NN} in 'Takanari' to 'Koshihikari' (E_{Taka}/E_{Koshi}). No data are included in the gray areas. In each panel, T_a and R_n were fixed as 25, 30, or 35 °C and 150, 450, or 750 W·m^{-2}, respectively. The time and RH were sequenced from 6:00 to 18:00 and 30 to 100%, respectively in all 9 patterns of panels.

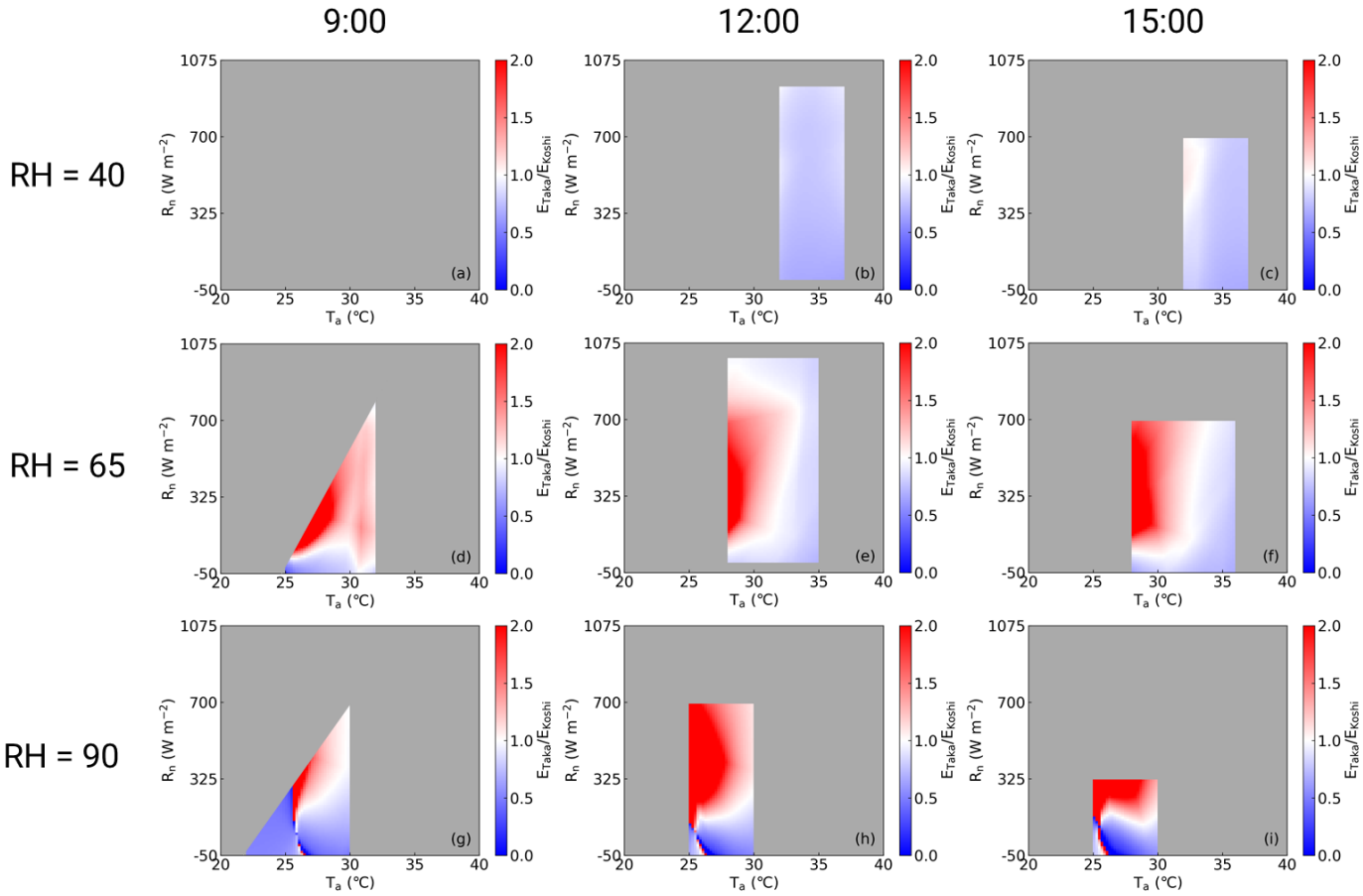

Fig. 4.9. Heatmap showing the varietal difference in the simulated values of canopy transpiration rate (E_{NN}) in 'Koshihikari' and 'Takanari'. Red, white, and blue represent the ratio of the simulated value of E_{NN} in 'Takanari' to 'Koshihikari' (E_{Taka}/E_{Koshi}). No data are included in the gray areas. In each panel, time and RH were fixed as 9:00, 12:00, or 15:00 and 40, 65, or 90%, respectively. The T_a and R_n were sequenced from 20 to 40 °C and -50 to 1075 W·m^{-2}, respectively in all 9 patterns of the panels.

According to the E_{NN} simulation, E_{NN} in ‘Takanari’ was generally higher than that in ‘Koshihikari’, mainly when T_a ranged from 25 to 30 °C and R_n was below 700 W m^{-2} (Figs. 4.8 and 4.9), which is comparable with the tendency of E in ‘Koshihikari’ and ‘Takanari’ displayed in Figs. 4.6 and 4.7. Such conditions are frequently and mainly observed in the morning. In the morning, solar radiation is gradually increasing, which means that plants are usually in a photosynthetic induction state. According to previous studies, the photosynthetic induction response to fluctuating light is faster in ‘Takanari’ than in ‘Koshihikari’, and this difference is mainly attributed to the difference in the temporal changes of stomatal conductance in the two cultivars (Adachi, Tanaka et al., 2019; Ohkubo et al., 2020; Taniyoshi et al., 2020). Our results are comparable with the reported characteristics of photosynthetic activity in these two cultivars.

‘Takanari’ showed a remarkably lower E_{NN} when T_a was higher than 33 °C, compared to ‘Koshihikari’ (Figs. 4.8 and 4.9); this finding was comparable to the tendency of E in ‘Koshihikari’ and ‘Takanari’ displayed in Figs. 4.6 and 4.7. This tendency might be mainly attributed to the sensitivity of the stomata to meteorological changes. In general, RH tends to be low under high-temperature conditions. A previous study reported that the stomatal conductance decreased more in ‘Takanari’ than in ‘Nipponbare’, a typical *japonica* cultivar, to drought stress (Ohsumi et al., 2008). Thus, the stomata in ‘Takanari’ are thought to be more sensitive to dry conditions than ‘Koshihikari’. These stomatal characteristics in ‘Takanari’ may have led to lower transpiration under such conditions, which was also observed in Chapter 3.

Many previous studies have reported that the saturated photosynthetic rate in a single leaf is greater in ‘Takanari’ than in ‘Koshihikari’ (Hirasawa et al., 2010; Takai et al., 2010; Adachi, Yamamoto et al., 2019; Taylaran et al., 2011). However, as mentioned

above, the genotypic variation observed in canopy transpiration between ‘Koshihikari’ and ‘Takanari’ depends on the meteorological conditions, both by the heat balance model and the neural network. In particular, the E in ‘Koshihikari’ was higher than that in ‘Takanari’ when T_a was over 33 °C and RH was under 52.5% (Fig. 4.6 and 4.7). In addition to the stomatal characteristics mentioned above, the canopy structure of the two cultivars may have caused this inconsistency. It was revealed that the leaf area distribution in ‘Takanari’ is denser than that in ‘Koshihikari’ while r_a under windless conditions in ‘Takanari’ is higher than that in ‘Koshihikari’ (Chapter 3). Such findings indicate that ‘Takanari’ has a canopy structure that tends to prevent gas diffusion compared to ‘Koshihikari’, which can partly mitigate the single leaf gas exchange of ‘Takanari’.

Chapter 5

General Discussion

5.1 Effects of the introduction of r_a* on the performance of the heat balance model

The aim of this study was to evaluate the canopy gas exchange under fluctuating meteorological conditions in field-grown rice. In the field, meteorological conditions are rapidly changing and affecting canopy gas exchange. Besides, canopy gas exchange is affected by plant factors such as canopy structure and mutual shading of leaves. Therefore, continuous monitoring was demanded for understanding realistic nature of canopy gas exchange. However, methods to evaluate canopy gas exchange under field conditions with sufficient stability and time resolutions was not established.

In Chapter 2, r_a*, the aerodynamic resistance under windless conditions, was directly measured and used for the modification of the heat balance model. A significant difference was detected among 7 genotypes. This difference may be attributed to canopy structure. The value of r_a* was correlated to leaf area density, which is represented by the ratio of leaf area index to canopy height. It is thought that the gas diffusion to the atmosphere is less likely to occur in a rice canopy with high leaf area density.

The serious problem in the original heat balance model was that it is unstable under low wind velocity, even though such a situation is frequently observed in field conditions. As a result of modification based on r_a*, the stability of the heat balance model to low wind velocity was remarkably improved. This means that the newly modified model in the present study is more applicable for continuous use in the field conditions compared to previous ones.

The technical difficulties in the measurements of r_a* remains as a major concern. Because the value of r_a* seems to be affected by canopy structures, additional measurements of r_a* are needed in different growth stages. However, in a canopy with lower leaf area and/or plant height, it is difficult to evaluate r_a*. After heading stage, the heat transfer from the air to a canopy is too complex for our measurement protocol because of the existence of panicles. As discussed later, the seasonal expansion is a prime task for the modified model. To achieve this objective, the improvement of the method for measuring r_a* is necessary.

5.2 Evaluation of canopy transpiration by the modified heat balance model

In Chapter 3, rice canopy transpiration in 7 genotypes was continuously estimated in 1-second intervals for 8 days. Because of the improvement of stability in the heat balance model, the estimation was successfully conducted. Continuous estimation with high time-resolution enabled evaluation of characteristics of canopy gas exchange in field grown rice. The *E* in 'Takanari' was remarkably higher than 'Koshihikari' in the morning, while comparable with 'Koshihikari' in the afternoon. This result implied that great photosynthetic capacity of a single leaf in 'Takanari' can be mitigated in canopies under hot or dry conditions. The significant correlations between hourly cumulative transpiration and final grain yield were detected, especially for transpiration from 9:00 to 12:00 on sunny days in the period of 1 week before heading. The amount of daily cumulative transpiration amount in high-yielding cultivars was higher than the other cultivars throughout the measurement. This result suggested that the continuous advantages of canopy gas exchange in the morning is important for yield formation in field-grown rice. On the other hand, the relationship between canopy transpiration and

biomass production was not directly discussed in this study. With this relationship cleared, far better understandings about rice canopy biomass production under fluctuating meteorological conditions may be gained.

In the field, the meteorological condition changes every seconds. Therefore, the heat balance equations may not precisely hold, and canopy surface temperature is in non-steady state. For the precise analysis of canopy heat balance, the transient heat balance should be taken account. However, establishing such model is limited by the spatial non-uniformity of wind velocity, accuracy of sensor devices and so on. Hence, we assumed the semi-steady state in terms of heat balance under changing weather conditions. As we discussed in Chapter 3, the value of g_c and E calculated by our modified model seems to be valid. Establishing more precise model considering transient heat balance should be conducted in the future studies.

A limitation of our study is that our method is not applicable after the heading stage. For example, it is reported that panicle temperature is higher than leaf temperature under sunny conditions in wheat (Ayaneh et al., 2002). Therefore, calculating leaf temperature from thermal images is difficult. Because biomass productivity after the heading stage affects yield and grain filling (Nagata et al., 2001; Ookawa et al., 2003; Takai et al., 2006), the development a method for estimating canopy transpiration after heading is also needed. For gaining better understandings of biomass production and yield formation in rice, further research for a seasonal expansion of our method is necessary.

5.3 Effects of the utilization of neural networks for evaluating rice canopy transpiration

In Chapter 4, the model to predict canopy transpiration rate only from

meteorological data was established based on the neural network for ‘Koshihikari’ and ‘Takanari’ grown under conventional management. The prediction accuracy was thought to be good enough when the estimation by the modified heat balance model was successfully conducted. It is notable that the accuracy of this prediction model was attributed to the size of datasets, which was provided by the newly modified heat balance model.

There are two important point for this model by the neural network. One is that it enables us to omit the measurement of r_a and T_c for E estimation/prediction. Although the measurement of r_a under field conditions has been attempted in many previous studies (Horie et al., 2006; Yasutake et al., 2006; Liu et al., 2007; Jones et al., 2018; Hou et al., 2019), many of them had problems in their labor and instrumental costs, stabilities, and time resolutions. The measurements of T_c are associated with remarkable costs and require a great deal of time. Further, their accuracy is markedly affected by the meteorological conditions, especially by wind velocity. Our model using the neural network showed good performance for the prediction of E_{NN} without these parameters. Another point is that our model revealed genotypic characteristics in responses of canopy transpiration to meteorological conditions. These characteristics have been masked mainly because of the instability and difficulties in estimations/measurements of canopy transpiration. It is thought that noises in the estimated values of E were successfully removed, which realized a monitoring of short-time fluctuations of canopy transpiration with practical accuracies. Therefore, our model is an option for estimating rice canopy transpiration in field environments using only meteorological data.

The sensitivity analysis of the model based on the neural network revealed a varietal difference in the response of canopy transpiration to the combinations of various

meteorological factors. The important suggestion was that the advantages in canopy transpiration was shown in different meteorological conditions between ‘Koshihikari’ and ‘Takanari’. This difference might be attributed to the characteristics of stomata in the two cultivars (Ohsumi et al., 2008; Adachi, Tanaka et al., 2019; Taniyoshi et al., 2020). The genotypic difference of physiological responses to meteorological conditions in two cultivars having contrastive photosynthetic characteristics was detected based on the predicted values of E_{NN}.

Our model, which is based on the neural network, has limitations. Briefly, this model is specific to two cultivars, ‘Koshihikari’ and ‘Takanari’, cultivated in Kyoto, Japan. Applications of our model to other cultivars, locations, cultivating systems are extremely limited. One option to overcome this limitation is to collect data on E for other cultivars and environments using the modified heat balance model. The versatility of this model may be improved by inputting newly collected data. However, collecting a comparable size of new data is a time-consuming task. To reduce labor costs for collecting new training data, fine-tuning may be useful. In fine-tuning, all the layers of the pre-trained model, besides the last layer, are essentially copied, and the last layer is replaced by a new layer that has weights for the new targets. Previous studies have reported that the same level of prediction performance as full training can be achieved with a reduced size of the dataset (Cetinic et al., 2018; Tajbakhsh et al., 2016; Howard & Ruder, 2018). Therefore, this technique may be useful for the genotypic, seasonal, and regional expansion of the model established in the present study.

5.4 Future perspectives of this study

The new methods shown in the present study may be useful for evaluating canopy

growth process and reactions of canopy gas exchange under various meteorological conditions in rice. Because our methods are now applicable only for field-grown rice, applications to other crop species (e.g., soybean, maize, wheat, and cotton) needs to be studied. To achieve this objective, the differences of canopy structure will be a challenging task. The further studies on methods for measuring r_a* and T_c must be conducted.

Nowadays, the climate change is a big concern for global societies. Under changing environments, field crops may show unknown growth. Our methods may be useful for evaluating crop growth in the future because they can investigate the relationships between rice canopy transpiration and combinations of meteorological factors in detail. For example, the global warming is steadily ongoing. Compared to 1850-1900 level, the average temperature of the world has risen 1.0 ℃ in 2014 and is expected to rise 1.5 ℃ in 2040 and, at maximum, 2.0 ℃ in 2060 (Masson-Delmotte et al., 2018). The effects of global warming on the production and yield of field crops remain unclear. According to Liu et al. (2019), probability of extreme low yield will increase in the scenario of 1.5 ℃ and 2.0 ℃ global warming. Raune et al. (2018) reported that the production of maize and rice will decrease 0-5 % in the global warming of 1.5 ℃, while Chen et al. (2018) reported that rice yield will slightly increase in the same scenario. To deal with uncertainties by the environmental changes, it will be necessary not only to investigate and predict final yield but also to monitor and evaluate growth and yield formation process in field-grown crops. The modified heat balance model in the present study may be useful because it can monitor the real-time dynamics of canopy transpiration under field conditions.

The combination of the methods in the present study and experimental treatments such as heat stress, drought stress, and CO_2 elevation are also worth evaluating.

Estimating canopy transpiration under such treatments by the modified heat balance model and imputing the data to the neural network may provide us better understandings and simulations of the growth of field crops under changing environments.

5.5 Conclusion

Modification of the heat balance model by the introduction of r_a* improved its robustness. The modified model enabled estimations of rice canopy transpiration with high time-resolution under field conditions. By the large amount of data obtained by the modified heat balance model, the model to predict rice canopy transpiration using only meteorological data was established based on the neural network. The methods developed in the present study will be useful for evaluating production process and its genotypic differences in rice canopies under field conditions.

Acknowledgments

I appreciate Dr. Koki Homma, a professor at the Graduate School of Agricultural Science, Tohoku University, for giving techniques to measure canopy surface temperature and meteorological data under field conditions. I am also grateful to Mr. Hiroto Katayama, a former member of the laboratory of crop science, Kyoto University, for helping to develop the method to measure r_a*. Dr. Tatsuhiko Shiraiwa, Dr. Tomoyuki Tanaka-Katsube, and Dr. Yu Tanaka have given me critical and important advice, suggestions, and ideas for conducting the present research throughout the activities in the laboratory of crop science. Ms. Hinaka Ito, Mr. Koshi Mitsuta, Mr. Shogo Ohashi, and Mr. Kota Nakajima helped me with the night-time experiment for measuring r_a*. I sincerely appreciate all of them. I must here say special thanks to Dr. Eiichi Kondo, a professor at Yamanashi University, and my father, with his academic opinion and economical supports for my research life.

References

Adachi, F., Kobata, T., Arimoto, M. & Imaki, T. (1995). Comparison of Water Use Efficiency in Paddy Rice (*Oryza sativa* L.) among Locations and Interannual Variations in Humid Areas. *Japan Journal of Crop Science*, 64, 509-515. (in Japanese with English summary)

Adachi, S., Yamamoto, T., Nakae, T., Yamashita, M., Uchida, M., Karimata, R., Ichihara, N., Soda, K., Ochiai, T., Ao, R., Ostuka, C., Nakano, R., Takai, T., Ikka, T., Kondo, K., Ueda, T., Ookawa, T. & Hirasawa, T. (2019). Genetic architecture of leaf photosynthesis in rice revealed by different types of reciprocal mapping populations. *Journal of Experimental Botany*, 70, 5131-5144.

Adachi, S., Tanaka, Y., Miyagi, A., Kashima, M., Tezuka, A., Toya, Y., Kobayashi, S., Ohkubo, S., Shimizu, H., Kawai-Yamada, M., Sage, R. F., Nagano, A. J. & Yamori, W. (2019). High-yielding rice Takanari has superior photosynthetic response to a commercial rice Koshihikari under fluctuating light. *Journal of Experimental Botany*, 70, 5287-5297.

Alberto, M. C. R., Wassmann, R., Buresh, R. J., Quilty, J. R., Correa, T. Q. Jr., Sandro, J. M. & Centeno C. A. R. (2014). Measuring methane flux from irrigated rice fields by eddy covariance method using open-path gas analyzer. *Field Crops Research*, 160, 12-21.

Anten, N. P. R. (1999). Modelling canopy photosynthesis using parameters determined from simple non-destructive measurements. *Ecological Research*, 12, 77-88.

Ayaneh, A., van Ginkel, M., Reynolds, M.P. & Ammar, K. (2002). Comparison of peduncle and canopy temperature depression in wheat under heat stress. *Field Crops Research*, 79, 173-184.

Beadle, C. L. & Long, S. P. (1985). Photosynthesis — is it Limiting to Biomass Production? *Biomass*, 8, 119-168.

Burkart, S., Manderscheid, R., Weigel, H. J. (2007). Design and performance of a portable gas exchange chamber system for CO_2- and H_2O-flux measurements in crop canopies. *Environmental and Experimental Botany*, 61, 25-34.

Carmo-Silva, A. E., Gore, M. A., Andrade-Sanchez, P., French, A. N., Hunsaker, D. J. & Salvucci M. E. (2012). Decreased CO_2 availability and inactivation of Rubisco limit photosynthesis in cotton plants under heat and drought stress in the field. *Environmental and Experimental Botany*, 83, 1-11.

Cetinic, E., Lipic, T. & Grgic, S. (2018). Fine-tuning Convolutional Neural Networks for fine art classification. *Expert Systems With Applications*, 114, 107-118.

Chang, S., Chang, T., Song, Q., Zhu, X. G. & Deng, Q. (2016). Photosynthetic and agronomic traits of an elite hybrid rice Y-Liang-You 900 with a record-high yield. *Field Crops Research*, 187, 49-57.

Chen, W., Yao, X., Cai, K. & Chen, J. (2011). Silicon Alleviates Drought Stress of Rice

Plants by Improving Plant Water Status, Photosynthesis and Mineral Nutrient Absorption. *Biological Trace Element Research*, 142, 67-76.

Chen, Y., Zhang, Z. & Tao, F. (2018). Impacts of climate change and climate extremes on major crops productivity in China at a global warming of 1.5 and 2.0 ℃. *Earth System Dynamics*, 9, 543- 562.

Choudhury, B. J. (1987). Relationships Between Vegetation Indices, Radiation Absorption, and Net Photosynthesis Evaluated by a Sensitivity Analysis. *Remote Sensing of Environment*, 22, 209-233.

Crafts-Brandner, S. J. & Salvucci, M. E. (2002). Sensitivity of Photosynthesis in a C4 Plant, Maize, to Heat Stress. *Plant Physiology*, 129, 1773-1780.

Das, B., Nair, B., Reddy, V. K. & Venkatesh P. (2020). Evaluation of multiple linear, neural network and penalised regression models for prediction of rice yield based on weather parameters for west coast of India. *International Journal of Biometeorology*, 62, 1809-1822.

De Souza, A. P., Wang, Y., Orr, D. J., Carmo-Silva, E. & Long, S. P. (2019). Photosynthesis across African cassava germplasm is limited by Rubisco and mesophyll conductance at steady state, but by stomatal conductance in fluctuating light. *New Phytologist*, 225, 2498-2512.

Drake, B. G. & Leadley P. W. (1991). Canopy photosynthesis of crops and native plant communities exposed to long-term elevated CO_2. *Plant, Cell and Environment*, 14, 853-860.

Evans, L. T. (1993). *Crop Evolution, adaptation and yield*. Cambridge: Cambridge University press. 1-514.

Fan, J., Zheng, J., Wu, L. & Zhang, F. (2021). Estimation of daily maize transpiration rate using support vector machines, extreme gradient boosting, artificial and deep neural networks models. *Agricultural Water Management*, 245, 106547.

Food and Agriculture Organization of the United Nations (FAO). (2019). FAOSTAT database. http://www.fao.org/faostat/en/#home. (Accessed June 8, 2021).

Gates, D. M. (1968). Transpiration and leaf temperature. *Annual Review of Plant Physiology*, 19, 211-238.

Haghverdi, A., Washington-Allen, R. A. & Leib, B. G. (2018). Prediction of cotton lint yield from phenology crop indices using artificial neural networks. *Computers and Electronics in Agriculture*, 152, 186-197.

Hamby, D. M. (1994). A review of techniques for parameters sensitivity analysis of

environmental models. *Environmental Monitoring and Assessment*, 32, 135-154.

Hirasawa, T., Ozawa, S., Taylaran, R. D. & Ookawa, T. (2010). Varietal Differences in Photosynthetic Rates in Rice Plants, with Special References to the Nitrogen Content of Leaves. *Plant Production Science*, 13, 53-57.

Hirooka, Y., Homma, K. & Shiraiwa, T. (2018). Parameterization of the vertical distribution of leaf area index (LAI) in rice (Oryza sativa L.) using a plant canopy analyzer. *Scientific Reports*, 8, 6387.

Horie, T., Matsuura, S., Takai, T., Kuwasaki, K., Ohsumi, A. & Shiraiwa, T. (2006). Genotypic difference in canopy diffusive conductance measured by a new remote-sensing method and its association with the difference in rice yield potential. *Plant, Cell and Environment*, 29, 653-660.

Horton, P. (2000). Prospects for crop improvement through the genetic manipulation of photosynthesis: morphological and biochemical aspects of light capture. *Journal of Experimental Botany*, 51, 475-485.

Hou, M., Tian, F., Zhang, L., Li, S., Du, T., Huang, M. & Yuan, Y. (2019). Estimating Crop Transpiration of Soybean under Different Irrigation Treatments Using Thermal Infrared Remote Sensing Imagery. *Agronomy*, 9, 8.

Howard, J. & Ruder, S. (2018). Universal Language Model Fine-Tuning for Test

Classification. arXiv:1801.06146v5.

Ikawa, H., Chen, C. P., Sikma, M., Yoshimoto, M., Sakai, H., Tokida, T., Usui, Y., Nakamura, H., Ono, K., Maruyama, A., Watanabe, T., Kuwagata, T. & Hasegawa, T. (2017). Increasing canopy photosynthesis in rice can be achieved without a large increase in water use—A model based on free-air CO_2 enrichment. *Global Change Biology*, 1-21.

Jin, X., Li, Z., Feng, H., Ren, Z. & Li, S. (2020). Deep neural network algorithm for estimating maize biomass based on simulated Sentinel 2A vegetation indices and leaf area index. *The Crop Journal*, 8, 87-97.

Johnson, I. R. & Thornley, H. M. (1984). A Model of Instantaneous and Daily Canopy Photosynthesis. *Journal of Theoretical Biology*, 107, 531-545.

Jones, H. G. (2014), *Plants and Microclimate* (3rd ed.). Cambridge: Cambridge University Press. 1-423.

Jones, H. G., Hutchinson, P. A., May, T., Jamali, H. & Deery, D. M. (2018). A practical method using a network of fixed infrared sensors for estimating crop canopy conductance and evaporation rate. *Biosystems Engineering*, 165, 59-69.

Kabaki, N. (1993). Growth and yield of *japonica-indica* hybrid rice. *Japan Agricultural Research Quarterly*, 27, 88-94.

Katsura, K., Maeda, S., Horie, T. & Shiraiwa, T. (2006). A Multichannel Automated Chamber System for Continuous Measurement of Carbon Exchange Rate of Rice Canopy. *Plant Production Science*, 9, 152-155.

Keating, B. A., Herrero, M., Carberry, P. S., Gardner, J. & Cole M. B. (2014). Food wedges: Framing the global food demand and supply challenge towards 2050. *Global Food Security*, 3, 125-132.

Khan, M. I. R., Iqbal, N., Masood, A., Per, T. S. & Khan, N.A. (2013). Salicylic acid alleviates adverse effects of heat stress in proline production and ethylene formation. *Plant Signaling & Behavior*, 8:11, e26374.

Khush, G.S. (2001). Green revolution: the way forward. *Nature Reviews Genetics*, 2, 815-822.

Kimura, H., Hashimoto-Sugimoto, M., Iba, K., Terashima, I. & Yamori, W. (2019), Improved stomatal opening enhances photosynthetic rate and biomass production in fluctuating light. *Journal of Experimental Botany*, 71, 2339-2350.

Laza, R. C., Peng, S., Sanico A. L., Visperas, R. M. & Akita, S. (2001). Higher leaf area growth rate contributes to greater vegetative growth of F_1 hybrids in the tropics. *Plant Production Science*, 4, 184-188.

Liu, S., Lu, L., Mao, D. & Jin, L. (2007). Evaluating parameterizations of aerodynamic

resistance to heat transfer using field measurements. *Hydrology and Earth System Sciences*, 11, 769-783.

Liu, B., Martre, P., Ewert, F., Porter, J. R., Challinor, A. J., Muller, C., Raune, A. C. et al. (2019). Global wheat production with 1.5 ℃ and 2,0 ℃ above pre-industrial warming. *Global Change Biology*, 25, 1428-1444.

Long, S. P., Zhu, X. G., Naidu, S. L. & Ort, D. R. (2006). Can improvement in photosynthesis increase crop yields? *Plant, cell and environment*, 29, 315-330.

Luo, H., He, L., Du, B., Pan, S., Mo, Z., Duan, M., Tian, H. & Tang, X. (2020). Biofortification with chelating selenium in fragrant rice: Effects on photosynthetic rates, aroma, grain yield quality and yield formation. *Field Crops Research*, 255, 107909.

Ma, J., Li, Y., Chen, Y., Du, K., Zheng, F., Zhang, L. & Sun, Z. (2019). Estimating above ground biomass of winter wheat at early growth stages using digital images and deep convolutional neural network. *European Journal of Agronomy*, 103, 117-129.

Mann, C. C. (1999). Crop scientists seek a new revolution. *Science*, 283, 310-314.

Masson-Delmotte, V., Zhai, P., Pörtner, H. O., Roberts, D., Skea, J., Shukla, P. R., Pirani, A., Moufouma-Okia, W., Péan, C., Pidcock, R., et al. (2018). Global warming of 1.5 C. In *An IPCC Special Report on the Impacts of Global Warming of. 2018 October 8*; IPCC: Geneva, Switzerland.

Monsi, M. & Saeki, T. (2005). On the Factor Light in Plant Communities and its Importance for Matter Production. *Annals of Botany*, 95, 549-567.

Monteith, J. L. (1977). Climate and the efficiency of crop production in Britain. *Philosophical Transactions of the Royal Society B*, 281, 277-294.

Monteith, J. L. (1995). A reinterpretation of stomatal responses to humidity. *Plant, Cell and Environment*, 18, 357-364.

Monteith, J. L. & Unsworth, M. H. (2013). *Principles of Environmental Physics* (4th ed.). Burlington, MA: Academic Press. 1-401

Morison, J. I. L. & Gifford, R. M. (1983). Stomatal Sensitivity to Carbon Dioxide and Humidity. *Plant Physiology*, 71, 189-796.

Mujahidin, S., Azhar, N. F. & Prihasto, B. (2021). Analysis of Using Regularization Technique in The Convolutional Neural Network Architecture to Predict Paddy Disease for Small Dataset. *Journal of Physics: Conference Series*, 1726, 012010.

Mutava, R. N., Prince, S. J. K., Syed, N. H., Song, L., Valliyodan, B., Chen, W. & Nguyen, H.T. (2015). Understanding abiotic stress tolerance mechanisms in soybean: A comparative evaluation of soybean response to drought and flooding stress. *Plant*

Physiology and Biochemistry, 86, 109-120.

Nagata, K., Yoshinaga, S., Takanashi, J. & Terao, T. (2001). Effects of Dry Matter Production, Translocation of Nonstructural Carbohydrates and Nitrogen Application on Grain Filling in Rice Cultivar, 'Takanari', a Cultivar Bearing a Large Number of Spikelets. *Plant Production Science*, 4, 173-183.

Nam, D. S., Moon, T., Lee, J. W. & Son, J. E. (2019). Estimating transpiration rates of hydroponically-grown paprika via an artificial neural network using aerial and root-zone environments and growth factors in greenhouses. *Horticulture, Environment, and Biotechnology*, 60, 913-923.

Nevavuori, P., Narra, N. & Lipping, T. (2019). Crop yield prediction with deep convolutional neural networks. *Computers and Electronics in Agriculture*, 163: 104859.

Ohkubo, S., Tanaka, Y., Yamori, W. & Adachi S. (2020). Rice Cultivar Takanari Has Higher Photosynthetic Performance Under Fluctuating Light Than Koshihikari, Especially Under Limited Nitrogen Supply and Elevated CO_2. *Frontiers in Plant Science*, 11, 1308.

Ohsumi, A., Hamasaki, A., Nakagawa, H., Homma, K., Horie, T. & Shiwaiwa, T. (2008). Response of Leaf Photosynthesis to Vapor Pressure Difference in Rice (Oryza sativa L) Varieties in Relation to Stomatal and leaf Internal Conductance. *Plant Production Science*,

11, 184-191.

Ohtaki, E. (1984). Application of an infrared carbon dioxide and humidity instrument to studies of turbulent transport. *Boundary-Layer Meteorology*, 29, 85-107.

Oishi, A., Tanaka, Y., Xu, Z. & Shiraiwa, T. (2015). Investigation of lines with high photosynthetic capacity among a population derived from a cross between an erect panicle rice and non erect panicle rice. *Abstracts of the 239th Meeting of the CSSJ*, 87. (in Japanese) https://doi.org/10.14829/jcsproc.239.0_87

Ookawa, T., Naruoka, Y., Yamazaki, T., Suga, J. & Hirasawa, T. (2003). A Comparison of the Accumulation and Partitioning of Nitrogen in Plants between Two Rice Cultivars, Akenohoshi and Nipponbare, at the Ripening Stage. *Plant Production Science*, 6, 172-178.

Peng, S., Khush G. S. & Cassman K. G. (1994). Evolution of the new plant type ideotype for increased yield potential. In K. G. Cassman (Eds.), *Breaking the yield barrier. Proceedings of a Workshop on Rice Yield Potential in Favorable Environments* (pp. 5-20). Los Banos: International Rice Research Institute.

Peng, S., Cassman, K. G., Virmani, S. S., Sheehy, J. & Khush G. S. (1999). Yield potential trends of tropical rice since the release of IR8 and the challenge of increasing rice yield potential. *Crop Science*, 39, 1552-1559.

Peng, S., Laza, R. C., Visperas R. M., Sanico A. L., Cassman, K. G. & Khush, G. S. (2000). Grain yield of rice cultivars and lines developed in the Philippines since 1966. *Crop Science*, 40, 307-314.

Peng, S. & Khush, G. S. (2003). Four decades of breeding for varietal improvement of irrigated lowland rice in the International Rice Research Institute. *Plant Production Science*, 6, 157-164.

Qu, M., Hamdani, S., Li, W., Wang, S., Tang, J., Chen, Z., Song, Q., Li, M., Zhao, H., Chang, T., Chu, C. & Zhu, X. (2016). Rapid stomatal response to fluctuating light: an under-explored mechanism to improve drought tolerance in rice. *Functional Plant Biology*, 43, 727-738.

R Core Team (2018). *R: A language and environment for statistical computing*. Vienna, Austria: R Foundation for Statistical Computing.

Raune, A. C., Antle, J., Elliott, J., Folberth, C., Hoogenboom, G., Mason-D'Croz, D. et al. (2018). Biophysical and economic implications for agriculture of + 1.5 and + 2.0 ℃ global warming using AgMIP Coordinated Global and Regional Assessments. *Climate Research*, 76, 17-39.

Salter, W. T., Merchant, A. M., Richards, R. A., Trethowan, R. & Buckley, T. N. (2019). Rate of photosynthetic induction in fluctuating light varies widely among genotypes of wheat. *Journal of Experimental Botany*, 70, 2787-2796.

Salvucci, M. E. & Crafts-Brandner, S. J. (2004). Inhibition of photosynthesis by heat stress: the activation state of Rubisco as a limiting factor in photosynthesis. *Physiologia Plantarum*, 120, 179-186.

Sakuratani, T. & Horie, T. (1985). Studies on evapotranspiration from crops. (1) On seasonal changes, varietal differences and the simplified methods of estimate in evapotranspiration of paddy rice. *Journal of Agricultural Meteorology*, 41, 45-55. (in Japanese with English summary)

Sebrin, S. P., Singh, A., Desai, A. R., Dubois, S. G., Jablonski, A. D., Kingdon, C. C., Kruger, E. L. & Townsend, P. A. (2015). Remotely estimating photosynthetic capacity, and its response to temperature, in vegetation canopies using imaging spectroscopy. *Remote Sensing of Environment*, 167, 78-87.

Shimadzu, S., Seo, M., Terashima, I. & Yamori, W. (2019). Whole Irradiated Plant Leaves Showed Faster Photosynthetic Induction Than Individually Irradiated Leaves via Improved Stomatal Opening. *Frontiers in Plant Science*, 10, 1512.

Shimono, H., Okada, M., Yamakawa, Y., Nakamura, H., Kobayashi, K. & Hasegawa, T. (2009). Genotypic variation in rice yield enhancement by elevated CO_2 relates to growth before heading, and not to maturity group. *Journal of Experimental Botany*, 60, 523-532.

Soleh, M. A., Tanaka, Y., Nomoto, Y., Iwahashi, Y., Nakashima, K., Fukuda, Y., Long, S.

P. & Shiraiwa, T. (2016). Factors underlying genotypic differences in the induction of photosynthesis in soybean [*Glycine max* (L.) Merr.]. *Plant, Cell and Environment*, 39, 685-693

Song, Q., Xiao, H., Xiao, X. & Zhu, X. G. (2016). A new canopy photosynthesis and transpiration measurement system (CAPTS) for canopy gas exchange research. *Agricultural and Forest Meteorology*, 217, 101-107.

Tajbakhsh, N., Shin, J. Y., Gurudu, S. R., Hurst, R. T., Kendall, C. B., Gotway, M. B. & Liang, J. (2016). Convolutional Neural Networks for Medical Image Analysis: Full Training or Fine Tuning? *IEEE Transactions on Medical Imaging*, 35, 1299-1312.

Takai, T., Yano, M. & Yamamoto, T. (2010). Canopy temperature on clear and cloudy days can be used to estimate varietal differences in stomatal conductance in rice. *Field Crops Research*, 115, 165-170.

Takai, T., Matsuura, S., Nishio, T., Ohsumi, A., Shiraiwa, T. & Horie, T. (2006). Rice yield potential is closely related to crop growth rate during late reproductive period. *Field Crops Research*, 96, 328-335.

Takai, T., Adachi, S., Taguchi-Shiobara, F., Sanoh-Arai, Y., Iwasawa, N., Yoshinaga, S., Hirose, S., Taniguchi, Y., Yamanouchi, U., Wu, J., Matsumoto, T., Sugimoto, K., Kondo, K., Ikka, T., Ando, T., Kono, I., Ito, S., Shomura, A., Ookawa, T., Hirasawa, T., Yano, M., Kondo, M. & Yamamoto, T. (2013). A natural variant of *NAL1*, selected in high-yield rice

breeding programs, pleiotropically increases photosynthesis rate. *Scientific Reports*, 3, 2149.

Tanaka, Y., Adachi, S. & Yamori, W. (2019). Natural genetic variation of the photosynthetic induction response to fluctuating light environment. *Current Opinion in Plant Biology*, 49, 52-59.

Tang, L., Gao, H., Hirooka, Y., Homma, K., Nakazaki, T., Liu, T., Shiraiwa, T. & Xu, Z. (2017). Erect panicle super rice varieties enhance yield by harvest index advantages in high nitrogen and density conditions. *Journal of Integrative Agriculture*, 16, 1467-1473.

Taniyoshi, K., Tanaka, Y. & Shiraiwa, T. (2020). Genetic variation in the photosynthetic induction response in rice (*Oryza Sativa* L.). *Plant Production Science*, 23(4), 513-521.

Taylaran, R. D., Adachi, S., Ookawa, T., Usuda, H. & Hirasawa, T. (2011). Hydraulic conductance as well as nitrogen accumulation plays a role in the higher rate of leaf photosynthesis of the most productive variety of rice in Japan. *Journal of Experimental Botany*, 62, 4067-4077.

Taylor S. H. & Long S. P. (2017). Slow induction of photosynthesis on shade to sun transitions in wheat may cost at least 21% of productivity. *Philosophical transactions of the Royal Society B*, 372, 20160543.

United Nations (2019). World Population Prospects 2019. https://population.un.org/wpp/.

(Accessed May 17, 2021).

Van Rossum, G. & Drake, F. L. (2009). *Python 3 Reference Manual*. Valley (CA): Create Space: Scotts.

Vialet-Charbrand, S. & Lawson, T. (2019). Dynamic leaf energy balance: deriving stomatal conductance from thermal imaging in a dynamic environment. *Journal of Experimental Botany*, 70, 2839-2855.

Wu., A., Hammer, G. L., Doherty, A., Caemmerer, S. & Farquhar, D. (2019), Quantifying impacts of enhancing photosynthesis on crop yield. *Nature Plants*, 5, 380-388.

Yamamoto, K. (2019). Distillation of crop models to learn plant physiology theories using machine learning. *PLoS ONE*, 14, e0217075.

Yamauchi, M. (1994). Physiological bases for higher yield potential in F_1 hybrids. In S.S. Virmani (Eds,). *Hybrid rice technology: New developments and future prospects* (pp. 71-80). Los Banos: International Rice Research Institute.

Yamori, W. & Hikosaka, K. (2014). Temperature response of photosynthesis in C_3, C_4, and CAM plants: temperature acclimation and temperature adaptation. *Photosynthetic Research*, 119, 101-117.

Yamori, W., Kusumi, K., Iba, K. & Terashima, I. (2016). Increased stomatal conductance induces rapid changes to photosynthetic rate in response to naturally fluctuating light conditions in rice. *Plant, Cell & Environment*, 43, 1230-1240.

Yamori, W., Kusumi, K., Iba, K. & Terashima, I. (2020). Increased stomatal conductance induces rapid changes to photosynthetic rate in response to naturally fluctuating light conditions in rice. *Plant, Cell and Environment*, 43: 1230-1240.

Yan, H. & Oue, H. (2011). Application of the two-layer model for predicting transpiration from the rice canopy and water surface evaporation beneath the canopy. *Journal of Agricultural Meteorology*, 67, 89-97.

Yang, W., Peng, S. & Laza, R. C. (2007). Grain Yield and Yield Attributes of New Plant Type and Hybrid Rice. *Crop Science*, 47, 1393-1400.

Yasutake, D., Kitano, M., Kobayashi, T., Hidaka, K., Wajima, T. & He, W. (2006). Evaluation of canopy transpiration rate by applying a plan hormone “abscisic acid”. *Biologia, Bratislava*, 61, 315-319.

Yin, Y., Li, S., Liao, W., Lu, Q., Wen, X. & Lu, C. (2010). Photosystem II photochemistry, photoinhibition, and the xanthophyll cycle in heat-stressed rice leaves. *Journal of Plant Physiology*, 167, 959-966.

Yoon, D. K., Ishiyama, K., Suganami, M., Tazoe, Y., Watanabe, M., Imaruoka, S., Ogura, M., Ishida, H., Suzuki, Y., Obara, M., Mae, T. & Makino, A. (2020). Transgenic rice overproducing Rubisco exhibits increased yields with improved nitrogen-use efficiency in an experimental paddy field. *Nature Food*, 1, 134-139.

Yoshida, S. (1972). Physiological aspects of grain yield. *Annual Review of Plant Physiology*, 23, 437-464.

Yuan, L. P. (1994). Increased yield potential in rice by exploitation of heterosis. In S.S. Virmani (Eds.), Hybrid Rice Technology. New Developments and Future Prospects (pp. 1-6). Los Banos: International Rice Research Institute.

Zhu, X. G., Long, S. P. & Ort, D. R. (2010). Improving Photosynthetic Efficiency for Greater Yield. *Annual Review of Plant Biology*, 61, 235-261.

Summary

Photosynthesis is the basic factor of the biomass production in field crops. In the field, crops are grown as canopy under fluctuating environmental conditions. To clarify the relationships between photosynthetic activity and biomass production under field conditions, measurements of canopy gas exchanges are needed. We have limited information about canopy photosynthetic activity and its genotypic differences because the conventional methods for measuring canopy photosynthesis because they require huge systems and many laborious costs. The objective of the present study was to evaluate the canopy gas exchange under fluctuating meteorological conditions for gaining better understandings of the process of biomass production under field conditions.

Canopy transpiration rate (E) can be estimated by dividing the vapor pressure deficit by the sum of the aerodynamic resistance (r_a) and the canopy diffusive conductance (r_c). In the heat balance model, it is assumed that the energy absorption is equaled to the sum of sensible heat flux and latent heat flux. The E and r_c can be estimated based on the meteorological data and parameters related to a canopy. However, it was difficult to apply the conventional heat balance model for estimating E and r_c under field conditions because r_a was assumed to be in inverse proportion to the wind velocity. Therefore, r_a under windless conditions (r_a*) was measured and used for the modification of the heat balance model to repress the divergence of r_a. In 2017, 7 genotypes including 'Koshihikari' and 'Takanari' was cultivated in the field. During the nighttime, a part of the canopy was surrounded by the silver sheet, and the heat was extracted from the infrared heater. Based on the subtraction of canopy surface temperature, r_a* was calculated. The r_a* was ranged from 9.50 s m^{-1} of 'Koshihikari' to 35.40 s m^{-1} of 'Takanari', and significant genotypic difference was detected. Besides, r_a* was significantly correlated to leaf area density, a

ratio of leaf area index to canopy height. Based on the measured values of r_a*, the heat balance model was modified. For modified and non-modified heat balance model, a sensitivity analysis to wind velocity and canopy temperature depression was conducted. As a result, the estimation of g_c was successfully conducted under wider range of conditions in the modified heat balance model, compared to the non-modified one. This result implied that the robust method for evaluating canopy gas exchange was established by the introduction of the concept of r_a* to the heat balance model.

Next, g_c and E were estimated under field conditions using the modified heat balance model. From July 18 to 25, 2017, meteorological data and canopy surface temperature (T_c) in the 7 genotypes were recorded in 1-second intervals and substituted for the modified heat balance model. As a result, g_c and E was successfully estimated with high stability and short time intervals. The diurnal change patterns of g_c and E were corresponding to the pattern of net radiation (R_n) and relative humidity. The daily cumulative transpiration was ranged from 2.33 to 10.29 kg m^{-2} d^{-1}, and its daily change pattern was corresponding to the pattern of daily cumulative R_n. Significant genotypic difference in the daily cumulative transpiration among the 7 genotypes was detected on all of the day for measurements. Hourly cumulative transpiration was significantly correlated to the final grain yield mainly from 9:00 to 12:00 on sunny days. Consequently, it is thought that the modified heat balance model in the present study enabled quantitative evaluation of rice canopy transpiration and its relationship between yield under field conditions.

The modified heat balance model has robustness against fluctuating meteorological conditions, especially against wind velocity. This enabled to collect large size of time-series data on E under field conditions. Based on the large size of datasets, the model to

predict E from only meteorological data was established using the neural network. The canopy characteristics and the modified heat balance model were substituted by the established model for the feature extraction of genotypic characteristics in the response of canopy transpiration to the meteorological conditions. From July 18 to 25, in 2018 and 2019, E was estimated using the modified heat balance model. Approximately 2,000,000 points of datasets in 'Koshihikari' and 'Takanari' were acquired throughout the 3-years measurements including 2017. Approximately 870,000 points of datasets in 'Koshihikari' were used for model establishment. After the model structure was decided, approximately 260,000 points of datasets in 'Koshihikari' and 'Takanari' were predicted. The predicted values were called E_{NN}. The prediction accuracy was represented by $R^2 = 0.76 \sim 0.85$ on sunny days. Therefore, it was thought that substitution of parameters representing canopy characteristics, T_c and r_a, and modified heat balance model can be substituted by neural network. The response of canopy transpiration to the meteorological conditions in 'Koshihikari' and 'Takanari' was evaluated by a sensitivity analysis. As a result, it was revealed that E_{NN} in 'Takanari' was higher than 'Koshihikari' under the conditions of air temperature from 25 to 30 ℃ and R_n under 700 W m^{-2}, while E_{NN} in 'Koshihikari' was higher under the conditions of air temperature around 35 ℃. Therefore, it was thought that 'Koshihikari' and 'Takanari' has advantages of canopy gas exchange under different conditions, which seemed to be affected by their stomatal characteristics.

The method in the present study can be used for the quantitative evaluation of rice canopy gas exchange and its relationships between yield, and meteorological conditions. Genotypic and seasonal expansions of this model may be useful for the effective evaluations of phenotypes related to grain yield under field conditions.

List of Publications

(Chapter 2 and 3)

Kondo, R., Tanaka, Y., Katayama, H., Homma, K. & Shiraiwa, T. (2021). Continuous estimation of rice (*Oryza Sativa* (L.)) canopy transpiration realized by modifying the heat balance model. *Biosystems Engineering*, 204, 292-303.

(Chapter 4)

Kondo, R., Tanaka, Y. & Shiraiwa, T. Prediction of rice canopy transpiration rate by neural networks and an evaluation of its response to various meteorological conditions. (*in preparation*)